www.sciencemag.org/content/357/6347/212/suppl/DC1

Supplementary Materials for

Germ line–inherited H3K27me3 restricts enhancer function during maternal-to-zygotic transition

Fides Zenk, Eva Loeser, Rosaria Schiavo, Fabian Kilpert, Ozren Bogdanović, Nicola Iovino*

*Corresponding author. Email: iovino@ie-freiburg.mpg.de

Published 14 July 2017, *Science* **357**, 212 (2017)
DOI: 10.1126/science.aam5339

This PDF file includes:

Other supplementary material for this manuscript includes the following:

Databases S1 to S4

Materials and Methods

Immunofluorescence

Ovaries and testes were dissected in 1X PBS + 0.05% BSA and fixed with 4% PFA in 1X PBS for 17 minutes (min) at room temperature.

For H3K27me3 staining, embryos were collected for 0-20 min or 0-120 min dechorionated, fixed with ice-cold methanol:heptane (1:1) and washed three times with ice-cold methanol.

For HA-staining, embryos were collected, dechorionated and transferred to 10 mL heptane before 5 mL of the fixative (4% PFA in 1X PBS) were added. After shaking the embryos for 20 min the aqueous layer was removed and 5 mL of methanol were added. After vortexing, the devitillinized embryos settled to the bottom of the tube and were ultimately washed three times with ice-cold methanol.

Subsequently the embryos (or ovaries and testes) were washed with 1X PBS + 0.2% Triton and blocked with 1% BSA before they were incubated for 2 h at room temperature (for H3K27me3) or overnight at 4 °C with the primary antibody. After washing with 1X PBS + 0.2% Triton, the secondary antibody and DAPI were incubated for another 2 h at room temperature. The embryos were then washed another four times with PBS + 0.2% Triton. VectaShield (Vector Laboratories H-1000) was used as mounting medium. The fly strains used for these experiments and their description is given in Table S1. All antibodies are listed in Table S2.

Imaging and Signal quantification

All images were acquired using the confocal laser scanning microscopes Leica TCS SP5 or Zeiss ELYRA PS1. Stacks were assembled using Fiji (*36*) or Imaris 8.1 (Bitplane).

For signal quantification the surfaces of the respective cells were manually assigned and the Intensity Sum was exported using Imaris 8.1. For plotting the signal, the intensity sum of the background was subtracted and the signal of the target was normalized to the DAPI signal.

Western Blot

Embryos were collected into Laemmli-Buffer (2 embryos per µL), sonicated (BioruptorPico, 10 cycles, 30 sec on/off) or crushed with a pestle, subsequently run on SDS-PAGE and transferred to PVDF membrane using Wet-Blot. 10 or 20 embryos were loaded per lane. The ECL signal was recorded using Amersham Hyperfilm ECL (GE Healthcare Life Sciences) or ChemiDoc Imaging System (Bio-Rad). All antibodies details are listed in Table S2.

Total RNA extraction for RNA-Seq and qPCR

Embryos were collected on apple juice agar plates and by using halocarbon oil 27 (Sigma 9002-83-9), they were staged under a stereoscope equipped with transmitted light. 25 hand-picked embryos were transferred into TRIzol Reagent (Ambion 12034977) and crashed with a small pestle. After chloroform extraction, the RNA was precipitated with Isopropanol, the pellet washed with 80% Ethanol and resuspended in TURBO™ DNase (Ambion AM2238) reaction mix. After inactivating the DNase the RNA was subjected to library preparation using the TruSeq Stranded Total RNA with Ribo-Zero Gold (Illumina) Kit or using the NEBNext rRNA depletion Kit (mouse/human/rat #E6310) followed by library preparation through the NEBNext Ultra Directional RNA Library Prep Kit for Illumina (#E7420). These libraries were generated starting from 1 µg of total RNA and amplified using 12-13 cycles of PCR. Alternatively the

RNA was used for cDNA synthesis (First Strand cDNA Synthesis, ThermoScientific #K1612) and following qPCR in a total reaction volume of 10 µL (FastStart Universal SYBR Green Master (Rox) Roche 04913850001 or Lightcycler FastStart SYBR Green Master 04673484001). (qPCR program: Preincubation: 600 sec at 95 °C, 2 Step Amplification: 15 sec at 95 °C, 60 sec at 60 °C – repeat 55x, Melting Curve: 15 sec at 95 °C, 60 sec at 60 °C, 1 sec at 95 °C, Cooling: 30 sec at 37 °C). Ct values were determined using the fitpoint method and then exported to further analyze the expression levels. The mRNA levels were normalized to the ribosomal gene RP49 and WT expression. Primers sequences are given in Table S3.

Embryo collection and ChIP-Seq

To enrich certain developmental stages, embryos were collected for 30 min on apple juice agar plates and aged at 25 °C according to the desired stage (cycle 9-13 for 70 min, cycle 14 for 140 min).

Dechorionated embryos were transferred to 10 mL heptane and crosslinked with 5 mL 1% PFA in buffer A (60 mM KCl, 15 mM NaCl, 15 mM HEPES [pH 7.6], 4 mM $MgCl_2$) for 15 min at room temperature on an orbital shaker. The crosslinking was stopped by the addition 225 mM glycine (final concentration) followed by incubation for 5 min. After washing with buffer A + 0.1% Triton, the embryos were hand-staged on a cooling station under a microscope with transmitted light according to their typical morphological traits.

During early development, all nuclei divide in the syncytial blastoderm. The number of cycles corresponds to the mitotic divisions. At cycle 9 the nuclei migrate to the periphery of the embryo and an initial subset of 100 genes is transcribed. The migration of the nuclei to the periphery of the embryo can be used as readout to follow the early developmental cycles. After 14 mitotic divisions the embryo is fully transcriptionally competent and membranes invaginate in between the nuclei. For a schematic representation see Fig. 2A and Fig. S1F.

Staged embryos were double-checked independently by two lab members and stored at -80 °C. For cycle 1-8 and 9-13, 1000-4000 embryos were used per experiment, for cycle 14, 400-700 embryos were used.

To extract the nuclei the embryos were transferred into Lysis buffer (140 mM NaCl, 15 mM HEPES [pH 7.6], 1 mM EDTA, 0.5 mM EGTA, 1 % TritonX100, 0.5 mM DTT, 0.1 % Sodium Deoxycholate, 10 mM Sodium Butyrate, 1X Protease Inhibitors) and subjected to ultrasound treatment (Covaris E220, 45 sec, peak power 75, duty factor 10, cycles burst 200). The nuclei were not pelleted nor washed; all following steps were conducted as described previously in (*6*), with slight changes regarding the shearing and chromatin precipitation starting at the lysis step. The chromatin was sheared using Covaris E220 (900 sec, peak power 140, duty factor 5, cycle burst 200). The quality of the shearing was inspected on a Bioanalyzer 2100 (Agilent). The chromatin was concentrated after elution using ChIP DNA Clean & Concentrator columns (Zymo Research). All antibodies and the used concentration are listed in Table S2.

Libraries were prepared according to manufacturer's instructions using the NEBNext Ultra DNA Library Prep Kit for Illumina and quality controlled on a Bioanalyzer 2100 (Agilent). Depending on the chromatin concentration of the Input between 12-14 cycles of PCR were performed to amplify the libraries. Sequencing was done using the HiSeq or NextSeq Illumina platform using the paired end sequencing option.

To control the ChIP assay, qPCR was performed in a total reaction volume of 10 µL. The signal of the IP was normalized to 1% and 10% of the Input to calculate the recovery (% Input). For the PCR program see Total RNA extraction for RNA-Seq and qPCR and primers are given

in Table S3. To validate targets by ChIP-qPCR time-staged embryos were collected (2:20-2:50 h after egg deposition). This time interval corresponds to cycle 14.

Phenotypical characterization of embryos and induction of RNAi in the female germline

To induce the RNAi- knock-down (KD), females carrying a transgene encoding the shRNA were crossed to males of the Gal4-driver. See Table S1 for further information on the fly lines. The progenies of this cross are KD for the target in the germline. This KD strategy overcomes the oogenesis defects that had previously hindered the functional analysis of chromatin modifiers in early embryogenesis. See Fig. 1A for a schematic depiction. The KD starts at around stage 3 of oogenesis and lasts until its end (arrow and red areas - in Fig.1A). In case of E(z)-KD, E(z) is still expressed in the *germarium* (green - in Fig. 1A). The oocyte is determined at stage 3 and stops cycling. By employing this strategy, late stage ovaries are devoid of E(z) mRNA and protein without interfering with meiosis, without affecting fertilization and without reducing the level of H3K27me3 on the oocyte, therefore enabling the study of early embryos devoid of E(z) mRNA and protein.

To determine the hatching rate of RNAi mediated E(z)-KD embryos, the embryos were collected for 0-1 h on apple juice agar plates. From the plates 50 embryos were randomly picked per experiment and transferred to a new plate in groups of 10. The hatching rate was calculated per group of 50 embryos and was plotted in a graph. The n gives the total number of embryos that were used in the experiment.

To complement this experiment we made use of a well-studied temperature sensitive allele of E(z) (E(z)-TS).Cages of flies homozygous for the E(z)-TS were kept at room temperature (permissive) and 29 °C (non-permissive). The embryos were collected for 0-3 h on apple juice agar plates, submerged with halocarbon oil 27 and embryos at cycle 14 (zygotic genome activation) were hand-picked. These embryos were transferred to a new apple juice plate in groups of 10. Per experiment 50-200 embryos were aligned per plate. The embryos were then left to develop for at least 30-36 h at either a permissive temperature, non-permissive temperature or they were shifted from the non-permissive temperature to a permissive temperature (referred to as shifted at ZGA). For each group the hatching-rate was calculated and is plotted in a graph, the n gives the total number of embryos that were used in the experiment.

For ChIP, western blot and cuticle preparations embryos that did not hatch after 36 h were picked, for the control that developed all the time at room temperature embryos were picked at stage 17 before hatching from the egg shell.

Cuticle preparation and characterization of homeotic transformation phenotype

Hand-picked embryos were manually dechorionated with 50% bleach in a dish. After washing the embryos with buffer A + 0.1% Triton they were transferred to a glass-slide and the remaining buffer was removed with tissue. The embryos were mounted in Hoyer's medium (30 g of gum arabic, 200 g of chloral hydrate, 20 ml of glycerol, 50 ml of distilled water) and incubated in a hybridization oven overnight at 65 °C. After all tissue had been dissolved the embryos were devitillinized by gently tapping the coverslip with a dissection needle.

The embryos were imaged using a dark field microscope. After scanning all slides the embryos were classified into one of five different groups based on the phenotype (homeotic transformation, other developmental defects, no phenotype/WT, no cuticle secreted, not classified).

Probe generation for in situ hybridization

Probes against the gene of interest were amplified from cDNA adding a T7 promoter with the forward primer and a T3 promoter with the reverse primer. Fragments of the corresponding size were subcloned into pJET 1.2 (Thermo Fisher Scientific, #K1232) and verified by sequencing.

To generate the probes, genes were PCR-amplified from plasmid DNA, purified and subjected to *in-vitro* transcription and DIG-labelling (Roche DIG RNA Labeling Mix, #11 277 073 910) following the manufacturer's instructions. Kr, kni and gt were *in-vitro* transcribed from linearized and purified plasmid DNA.

After DNase digestion and clean-up, the samples were subjected to alkaline hydrolysis to a final probe length of 500-800 bp (60 mM Na2CO3, 40 mM NaHCO3 final concentration at 60 °C). The reaction was stopped by adding 50 mM sodium acetate and 0.2% glacial acetic acid (final concentrations). After clean-up, the probes were stored at -80 °C until further use.

In situ hybridization

The embryos were fixed as described for immunofluorescence staining using 4% of PFA and stored at 20 °C in methanol until further use.

For the in situ hybridization the embryos were transferred into Roticlear (Carl Roth, CAS #64742-48-9) and washed on a rocker for 10 min. Afterwards the embryos were transferred back to 100% methanol, rinsed twice with permeabilization buffer (0.05% deoxicholic acid, 7.5 mM Tris-HCl [pH 8.8], 0.05% Saponin, 0.2% BSA, 0.1% TritonX100, 0.05% NP40) and ultimately incubated for 2 h at 4 °C in permeabilization buffer on a nutator.

Subsequently the embryos were fixed again with 4% PFA for 20 min at RT and then washed five times in 1xPBS+0.1% Triton. After the last wash the embryos were incubated for 10 min on a nutator in a 1:1 mixture of 1xPBS+0.1% Triton and hybridization buffer (1% Roche blocking reagent #11096176001, 0.1% CHAPS, 50% formamide, 5x SSC, 1x Denhardt's solution, 0.01% Herring sperm DNA (100 µg/ml), 0.01% Heparin (100 µg/ml), 0.1% Tween20). Before adding the probe, the embryos were incubated for 1-2 h at 56 °C in hybridization buffer. The probe was denatured to prevent secondary structures at 90 °C, snap cooled and added at a final concentration of 2 ng/µl in hybridization buffer to the embryos. The embryos were then incubated overnight at 56 °C. The next day the probe was removed and the embryos rinsed in hybridization buffer, before they were washed four times for 15 min at 56 °C. Another wash in a 1:1 mixture of 1xPBS+0.1% Triton and hybridization buffer was performed (15 min at RT on a nutator) before the embryos were washed another five times for 5 min in 1xPBS+0.1% Triton at room temperature. Next the embryos were blocked with 5% BSA in 1xPBS+0.1% Triton for 1 h on the nutator. Finally the α-DIG antibody was added diluted 1:500 with 1.5% BSA in 1xPBS+0.1% Triton. The antibody was incubated for at least two hours or overnight. Afterwards the embryos were washed five times for 10 min 1xPBS+0.1% Tween. To develop the staining, the embryos were washed three times for 5 min in AP-wash buffer (0.1 M Tris-HCl [pH 9.5], 0.1 M NaCl, 50 mM MgCl2, 1 mM Tetramisol, 0.1% Tween20). At last freshly prepared AP color (0.1 M Tris-HCl [pH 9.5], 0.1 M NaCl, 0.1% Tween20, 0.45 mg/ml NBT, 0.175 mg/ml) was added to the embryos. After the staining was revealed the reaction was stopped by washing the embryos in 1xPBS+0.1% Tween. Before mounting the embryos were rinsed 4 times with 100% Ethanol, once with 1xPBS+0.1% Tween and ultimately kept in 50% glycerol. For in-situ hybridization in contrast to the cuticle preparation embryos of the E(z)-TS were not shifted by

hand. They were collected for 1 h at a non-permissive temperature, aged for another 2 h and then shifted to the permissive temperature were they developed for at least another 5 h before they were fixed to perform the staining.

Cloning and generation of transgenic flies

The H3.3-FLAG-HA transgenes were amplified from cDNA using the primers FZ80_cacc_H3.3A_fw and FZ83_H3.3A_FLAG-HA_rev. The reverse primer added the FLAG-HA tag. After subcloning into the pENTRY vector the K27M mutation was added through the primer pair FZ81_H3.3A_K27M_fw and FZ82_H3.3A_K27M_rev. The restriction sites BamHI and SpeI, to clone the fragment into the pUASp-AttB vector (DGRC #1358, (*37*)), were added by another PCR step using the primer pair VA01_SpeI_H3.3_fw and VA02_HA_BamHI_rev.

To generate an alternative shRNA targeting E(z) the primers FZ028 shRNA 3UTR e(z) topstrand and FZ029 shRNA 3UTR e(z) bottomstrand were designed and annealed, strictly following the instructions published by the TRiP project (Transgenic RNAi project, http://fgr.hms.harvard.edu/cloning-and-sequencing (*38*)) and ligated with the NheI/EcoRI digested vector pVALIUM20 (*39*). All constructs were verified by sequencing and injected into *Drosophila* embryos.

Rescue of E(z)-KD embryos by zygotic overexpression

We asked whether overexpression of E(z) from the paternal genome could rescue the strong phenotype of E(z)-KD embryos. For this we used overexpression of E(z) through the tubulin promoter (*40*). The construct tubulin>GFP:E(z) results in 3 copies of E(z) and strong overexpression, this line was also used in Fig. S3A). The fly strains used for this experiment and their description is given in Table S1.

ChIP-Seq data analysis

Paired-end reads were mapped to the *Drosophila* genome (dm3 assembly) using bowtie2 (2.2.3) (*41*) and standard parameters. Alignments in SAM format were converted to BAM, sorted and deduplicated using sambamba v0.6.4 (PMID:25697820). Proper pairs were extracted with samtools (v0.1.19) (*42*) (flag 0x2) and used for downstream analyses. Peak calling was performed using MACS2 (*43*) using –g dm while leaving the remaining parameters at default values. Downstream analysis was largely performed using R (R Core Team, 2014; http://www.Rproject.org/) and BioConductor(*44*); http://www.bioconductor.org). Normalization of H3K27ac and H3K4me1 ChIP-Seq data was performed as outlined in (*45*) with the following modifications: for each sample, the background constants were computed on all 1 kb windows not overlapping with peaks. Furthermore, the foreground constants were set to 0.9-percentiles of the background subtracted read count distributions across 1 kb windows centered over all peaks. Metaprofiles and heatmaps were computed using the R package genomation (*46*). GO analysis was performed using the R package ChIPseeker (*47*).

For Fig. S4N ChIP data from modEncode was used to also investigate the H3K27ac at other developmental stages during embryogenesis. See Database S4 for further details.

Ordering H3K27ac peaks

To identify H3K27ac peaks with differential activity between E(z)-KD and wild type conditions the union over all H3K27ac peaks was computed and the number of reads falling into each resulting union peaks was counted. Significant differences between wild type and E(z)-KD were

determined using DESeq2 (*48*). Based on the DESeq2 results, the H3K27ac peaks were ordered by i) sign of log2FC and ii) p-values such that smallest p-values associated with positive log2FCs and negative log2FCs are at the top (gained in E(z)-KD) and the bottom (lost in E(z)-KD) of the list, respectively. The identified regions were then visually inspected for gain in H3K27ac.

Detection of H3K27me3 enriched domains

Processed reads for multiple experiments (see Database S4 -1 for further information) (both H3K27me3 and corresponding input) were merged using SAMtools (merge). Enriched H3K27me3 domains were called using the EDD algorithm (*49*) with an FDR of 0.05. Only domains displaying less than 20% genomic overlap with the UCSC repeatmasker track (*50*) were used for further analysis.

Data visualization

For data visualization, only reads mapping to unique genomic positions were selected. The visualization was performed using deepTools (*51*) bamCompare function to obtain log2 ChIP/input signal. All ChIP-seq experiments were performed in at least two biological replicates. For visualization the union of the tracks is shown in Fig. 2B.

Venn diagrams

The genomic overlaps between different sets of H3K27me3 enriched domains were obtained using BEDtools v2.17.0 (*52*). The Venn diagrams were constructed using the Venn diagram online tool (http://www.cmbi.ru.nl/~timhulse/venn/)

Sequencing, postprocessing, and RNA-seq analysis

The sequencing of the paired-end RNA-seq libraries was handeled by the MPI-IE sequencing facility on an Illumina sequencer. Its raw data was directly postprocessed according to the MPI-IE bioinformatics standards (BCL2Fastq pipeline v0.2), which include demultipexing and conversion into FASTQ files (Illumina bcl2fastq2 v1.8.4, http://support.illumina.com/downloads/bcl2fastq_conversion_software_184.html), contamination screening (fastq_screen v0.5.1, http://www.bioinformatics.babraham.ac.uk/projects/fastq_screen/), and quality control (FastQC v0.11.3, http://www.bioinformatics.babraham.ac.uk/projects/fastqc/). The project specific RNA-seq analysis performed trimming of low quality reads and sequencing adapters (Trim galore!, http://www.bioinformatics.babraham.ac.uk/projects/trim_galore/), library and insert size estimation (RSeQC v2.6.1,(*53*)), mapping (TopHat2 v2.0.13,(*54*)), counting of mapped reads (featureCounts subread-1.5.0-p1,(*55*)), and differential expression analysis (DESeq2 v1.10.1,(*48*)). SAMtools v1.2 (*42*) was used to handle (index, sort, filter) BAM files and allowed to combine all steps in a one stop pipeline (rna-seq-qc v0.8.3, https://github.com/kilpert/rna-seq-qc), which also serves as the resource for chosen software parameters. Ensembl (BDGP5, dm3, http://dec2014.archive.ensembl.org/Drosophila_melanogaster/Info/Index) served as reference for mapping and counting.

To analyze additional stages of *Drosophila* development in Fig. S4O, RNA-expression data from modEncode was used (*56*). These datasets were made accessible through the HiC browser (http://chorogenome.ie-freiburg.mpg.de/) (*57*).

Database S4 contains an overview over all samples subjected to RNA-sequencing.

Fig. S1 The intergenerational transmission of the repressive H3K27me3 mark does not require the enzymatic activity of E(z).

A: Testis of *Drosophila* stained for α-H3K27me3 and DAPI. The H3K27me3 mark is not detectable on the highly condensed sperm nuclei (filled arrowhead). Sperm nuclei can be easily recognized by the needle-shaped structure. H3K27me3 is still detectable on maturing sperm nuclei, earlier in development (open arrowhead). The arrow shows the direction of maturation, during which histones are replaced by protamines. The asterisk in contrast marks a somatic cell of the surrounding tissue that shows H3K27me3 staining. Scale bar 50 µm.

B: α-H3K27me3, α-H4ac and DAPI staining of the apposed pronuclei in the 1-cell wild type embryo. H3K27me3 is transmitted to the embryo through the maternal gamete. H4ac specifically stains the paternal pronucleus at this stage. Scale bar 2 µm.

C: qPCR of unfertilized eggs showing very strong reduction of *E(z)* mRNA upon RNAi-KD (mean±SD, $p=1.8\ e^{-005}$, t-test). Before zygotic genome activation, when the embryonic chromatin is still quiescent, the embryos rely solely on maternally loaded mRNA and protein. For this reason unfertilized eggs can be used to control the maternal load of protein and mRNA into the embryo.

D: Western blot showing that the endogenous E(z) is not detectable in unfertilized eggs laid by E(z)-KD females. 15 eggs were loaded per lane. α-tubulin and unspecific *Ponceau*-stained bands served as loading controls. E(z) protein and mRNA are maternally loaded into the embryos. After zygotic genome activation, at cycle 14, E(z) mRNA and protein are produced zygotically by the embryos.

E: Quantification of IF-detected H3K27me3 signal on the oocyte of WT and E(z)-KD females showing that E(z)-KD at late stages of oogenesis does not reduce H3K27me3 levels in the oocyte. The histone methyltransferase *E(z)* is depleted through RNAi only at late stages of oogenesis, when the oocyte has already entered prophase I of meiosis and is no longer cycling (Fig. 1A - red area), thereby H3K27me3 is not diluted out. This knock-down strategy overcomes the oogenesis defects that had previously hindered the functional analysis of chromatin modifiers in early embryogenesis. By employing this strategy, late stage ovaries are devoid of E(z) mRNA and protein without interfering with meiosis, without affecting fertilization and without reducing the level of H3K27me3 on the oocyte therefore enabling the study of early embryos devoid of E(z) mRNA and protein. The plotted signal is background subtracted and normalized to DNA content (DAPI signal) (mean±SD, p=0.7, Mann-Whitney test).

F: Overview of the time-course of *Drosophila* embryogenesis. During the embryonic phases, the embryos are staged by the number of mitotic divisions they have undergone (referred to as cycle 1-14). Around 170 min after egg deposition (AEG) the embryos have activated their genome and are fully transcriptionally competent. After ZGA, gastrulation starts at around stage 6. The germband is fully extended between stage 9 (around 3.5 h AEG) and stage 11 and starts to retract at stage 12 (around 7.5 h AED).

Supplement Figure 1

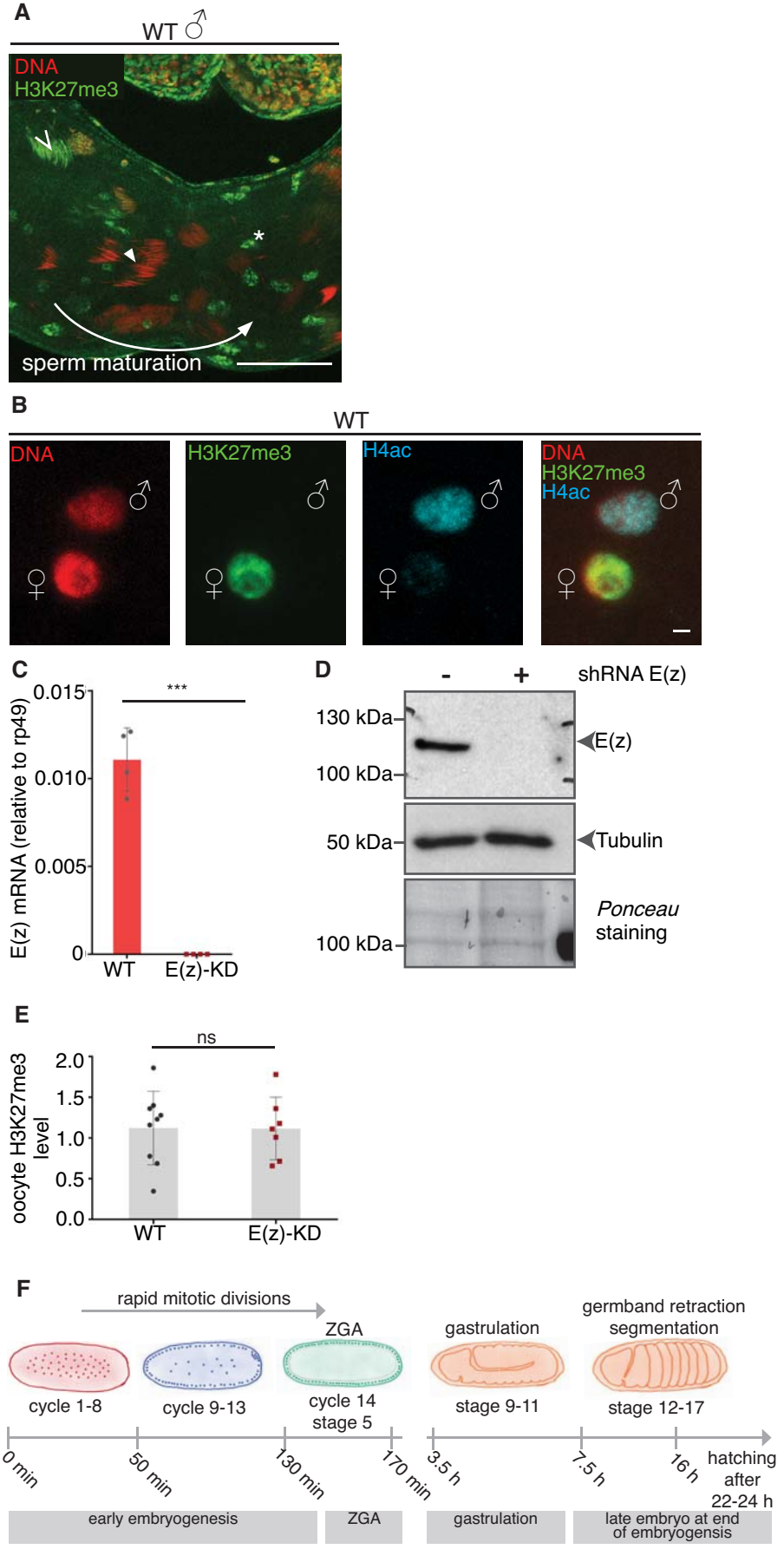

Fig. S2 Establishment of chromatin marks in developing *Drosophila* embryos

A: α-H3K27me3 (antibody from T. Jenuwein) and DAPI staining of different developmental cycles of a *Drosophila* WT and E(z)-KD embryo. H3K27me3 is actively propagated on the pluripotent nuclei before zygotic genome activation. For a better representation mitotic chromosomes are shown for cycle 2-10. H3K27me3 is reduced to a level undetectable by IF in E(z)-KD embryos, confirming the specificity of the antibody and the requirement of maternal E(z) for the propagation of H3K27me3. The images correspond to Fig. 1D-E and are shown here unmerged for clarity. Scale bar 2 μm.

B: α-HA staining of different developmental cycles of a *Drosophila* WT (HA-E(z)) and E(z) KD embryo. The speckled distribution of HA-E(z) from cycle 6 resembles Polycomb bodies. HA-E(z) cannot be detected on the chromatin upon E(z)-KD, confirming the specificity of the antibody. The images correspond to Fig. 1F-G and are shown here unmerged for clarity. Scale bar 2 μm.

C: α-H3K27me3 staining of a *Drosophila* WT embryo between mitotic cycle 10-13 using a commercial antibody from Millipore (07-449). For a better representation mitotic chromosomes are shown. Scale bar 2 μm.

D: α-H3K27me3 staining of a *Drosophila* WT embryo between mitotic cycle 10-13 using a commercial antibody from Diagenode (C15200181-50). For a better representation mitotic chromosomes are shown. Scale bar 2 μm.

E: α-H3K27ac and DAPI staining of wildtype early embryos at different developmental cycles, showing that H3K27ac only becomes detectable after around 8 nuclear divisions. Scale bar 20 μm.

F: α-H3K4me1 and DAPI staining of wildtype early embryos at different developmental cycles, showing that H3K4me1 only becomes detectable after around 11 nuclear divisions. Scale bar 20 μm.

G: α-H3K4me3 and DAPI staining of wildtype early embryos at different developmental cycles, showing that H3K4me3 only becomes detectable after around 14 nuclear divisions coinciding with the major wave of zygotic transcription at ZGA. Scale bar 20 μm.

H: Western blot of lysates from WT and E(z)-KD embryos to verify the specificity of different H3K27me3 antibodies. Also an H3K27me2 antibody was included, to test whether the E(z)-KD would also affect this histone modification.

I: Biological replicates of ChIP-tracks using different H3K27me3 antibodies, on embryos between cycle 9-13. The first and the last tracks show two biological replicates using the α-H3K27me3 from Diagenode. The second ChIP track was generated using α-H3K27me3 antibody from the lab of T. Jenuwein. All tracks are scaled from -0.5 to 0.6 and show the log2-fold change of the H3K27me3 IP over the input. In all tracks a clear enrichment of H3K27me3 on the HOX-cluster is detected (inset, *bxd*, *Ubx* and *abd-A*).

Supplement Figure 2

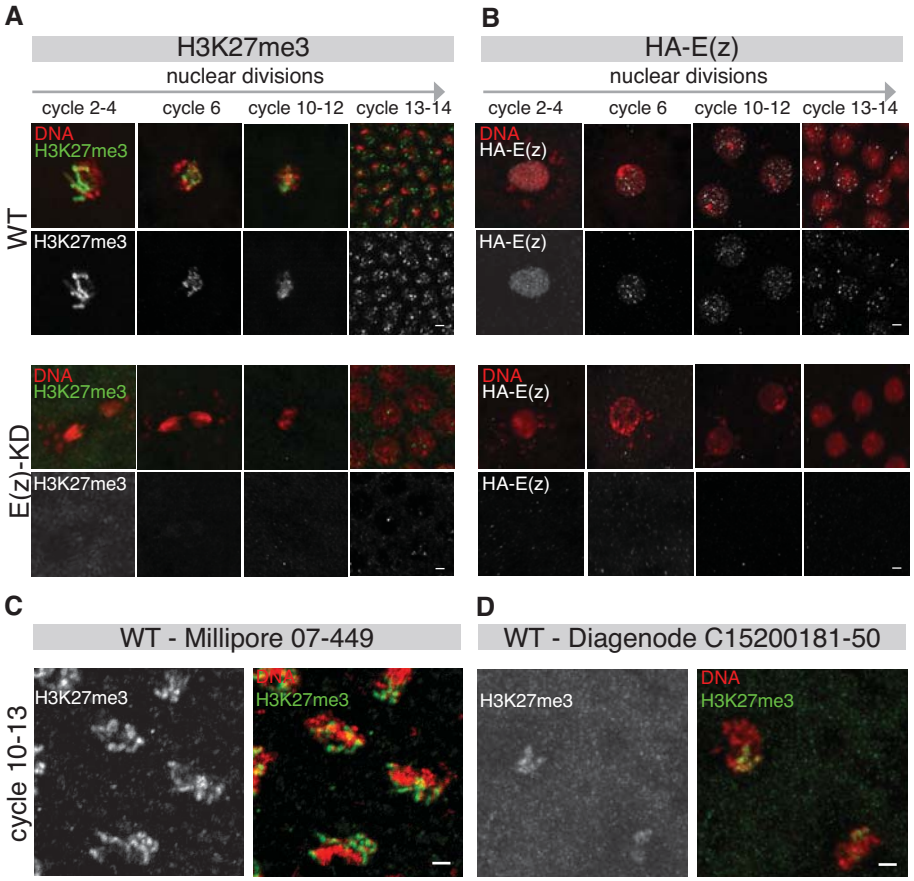

Supplement Figure 2

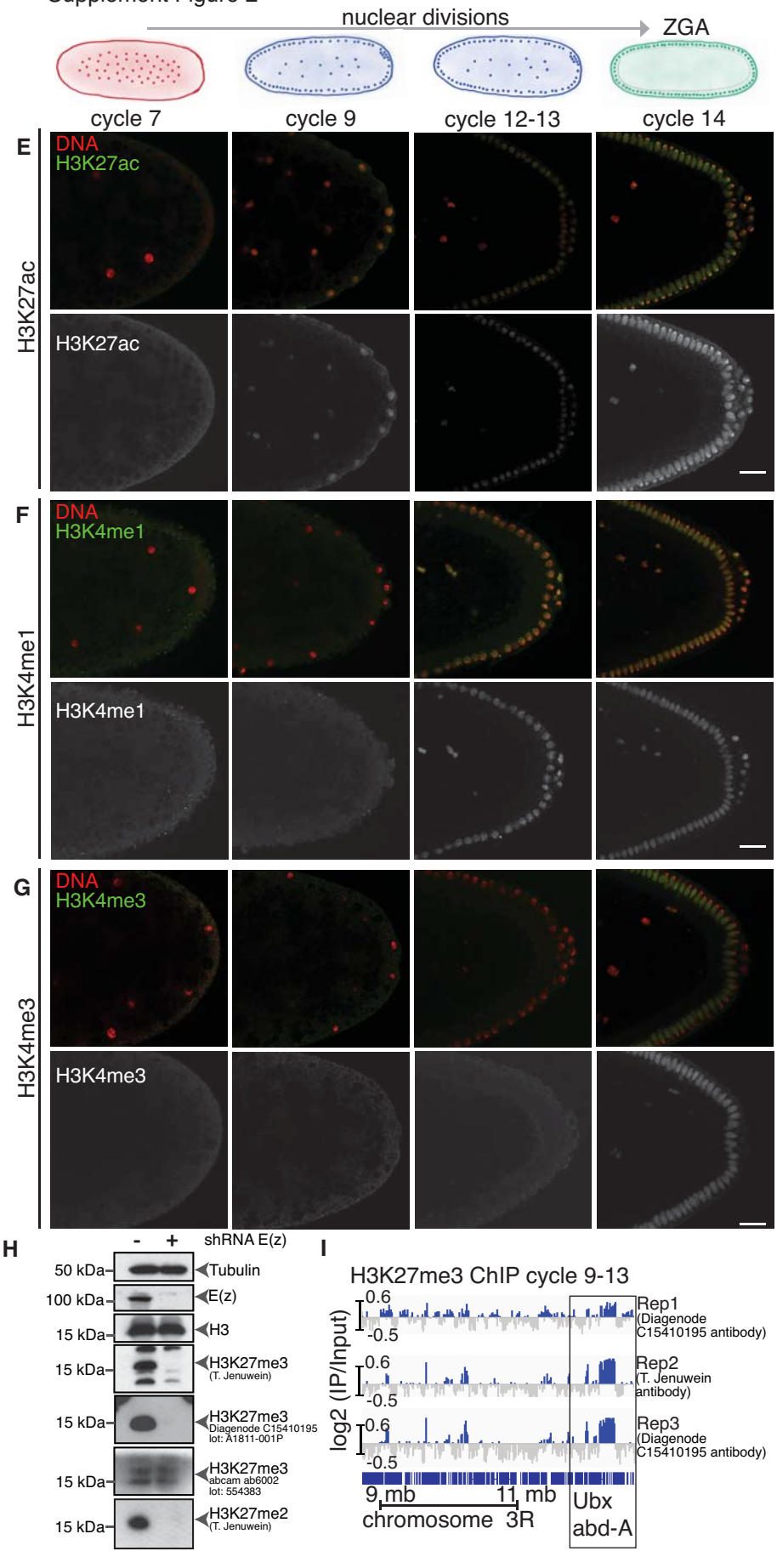

Fig. S3 Maternal KD of E(z) or loss of H3K27me3 before zygotic genome activation leads to embryonic lethality and homeotic transformation.

A: Characterization of the hatching rate of embryos depleted of maternal E(z) protein through a shRNA generated in this study (shRNA 1)(see also Fig. 3A, where a different hairpin, generated by the TRiP project, was used (shRNA 2)). The hatching rate results obtained from both shRNAs are very similar, although the hairpin generated in this study still shows an average hatching rate of 3%. The embryonic lethality can only be partially rescued by overexpressing E(z) from the paternal allele at ZGA. Overexpression of GFP-E(z) from a tubulin promoter only enhances the survival to 20%. This number is comparable to the embryonic survival observed in E(z)-TS embryos that were shifted to a permissive temperature at ZGA (Fig. 3C). All countings were performed in replicate. The n refers to the total number of embryos that were aligned. All fly lines used in this study are submitted in Table S1.

B: Western Blot on different concentrations of protein extract from WT and E(z)-KD before-ZGA embryos laid by females expressing either of the two shRNAs at late stages of oogenesis. Both hairpins deplete E(z) protein to a level undetectable by western blot.

C: Depletion of E(z) with either of the two shRNAs results in homeotic transformation of all anterior segments toward the most posterior segment A8.

D: *Drosophila* embryos at zygotic genome activation. The embryos are stained by *in-situ* hybridization with antisense probes recognizing *caudal* (cad) and *hunchback* (hb) mRNA. Both mRNAs are maternally loaded into the embryo and show comparable patterns in WT and E(z)-KD embryos.

E: Embryos stained by *in-situ* hybridization with antisense probes against the transcripts of the gap genes *giant* (gt), *knirps* (kni) and *krueppel* (Kr). The products of gap genes divide the embryo into broad domains, these show no difference between WT and E(z)-KD embryos.

F: Embryos stained by *in-situ* hybridization with antisense probes against *zerknullt* (zen) and *teashirt* (tsh). Both transcripts localize in particular patterns in the embryos. *Zen* only localizes to the dorsal side of the embryo while *tsh* localizes to the abdominal parts of the embryo. The patterns are indistinguishable between WT and E(z)-KD embryos.

G: Embryos stained by *in-situ* hybridization with antisense probes against the transcripts of the pair rule genes *even skipped* (eve), *fushi tarazu* (ftz), *hairy* (h), *odd skipped* (odd), paired (prd), *sloppy paired 1* (slp1). Pair rule gene patterning precedes segmentation and follows the pattern of the gap genes. The expression of pair rule genes defines segments during this intermediate stage with double periodicity.

H: Embryos stained by *in-situ* hybridization with antisense probes against the segment polarity gene *wingless* (wg). Segment polarity genes start to be expressed toward the end of stage 5. They maintain the striped pattern, defined by the gap and pair rule genes, later in development. There are no detectable differences between WT and E(z)-KD embryos comparing the expression pattern of wg.

I: Examples of loci that regain H3K27me3 at stage 17 (towards the end of embryogenesis) in WT and E(z)-TS shifted embryos (shifted at ZGA). For explanation of *Drosophila* embryogenesis see Fig. S1F. The H3K27me3 WT track was generated in (*58*).

J: Heat map of H3K27me3 clustered on EDs detected in embryos at the end of embryogenesis (n=226). The signal of WT and E(z)-TS embryos that were shifted back to a permissive temperature at ZGA is centered on the EDs in a 100 kb window. For explanation of *Drosophila* embryogenesis see Fig. S1F. The H3K27me3 WT ChIP data was generated in (*58*).

K: H3K27me3 ChIP-Seq tracks showing a window of chromosome 3R from different developmental stages of *Drosophila* embryos. For all stages H3K27me3 log2-enrichment over input is plotted and scaled from -0.5 to 1.77. The last track shows the H3K27me3 signal in E(z)-TS embryos at ZGA at a non-permissive temperature.
L: ChIP-qPCR of time staged embryos at around ZGA to determine the enrichment of H3K27me3 in the upstream region of H3K27me3-target (*gcm2*, *homeobrain* (hbn), *intermediate neuroblasts defective* (ind)) and non-target (*peptidoglycan recognition protein LE* (pgrp), *ribosomal protein L19* (rpl19) genes in WT, E(z)-KD and E(z)-TS embryos at permissive and non-permissive temperature. This shows that H3K27me3 levels are overall reduced in E(z)-TS and E(z)-KD embryos. In E(z)-TS embryos some small enrichment of H3K27me3 is still detectable at the non-permissive temperature.
M: Classification of embryonic phenotypes resulting from maternal loss of E(z) enzymatic function. Cuticles prepared from E(z)-TS embryos shifted from a non-permissive to a permissive temperature at ZGA were characterized and scored. Embryos that developed entirely at a permissive temperature were analyzed as a control.
Embryos developed at a permissive temperature show a WT cuticle pattern. Embryos that were shifted to a permissive temperature at ZGA exhibit various degrees of homeotic transformation. The severity was assessed by the lack of head-involution (referred to classical homeotic). Embryos that showed a homeotic cuticle pattern but also head involution, are referred to as homeotic head. (See also Fig. 3E).
N: Comparison of the expression of the HOX-genes *Ubx* and *Abd-B* throughout development. RPKM for the respective gene are plotted for WT and E(z)-TS embryos that were shifted at ZGA and E(z)-KD embryos. Upregulation of *Abd-B* in embryos that were shifted or are maternally depleted of E(z) can be observed from stage 11 onwards (after gastrulation). Consistent with the phenotype affecting only 50% of the shifted embryos the overexpression of *Abd-B* is reduced compared to E(z)-KD embryos. While *Abd-B* stays upregulated in E(z)-KD embryos, the expression of *Ubx* starts to decrease from stage 15 to stage 17 (end of embryogenesis) onwards. This is probably due to suppression by the more posterior HOX-gene *Abd-B*. For explanation of *Drosophila* embryogenesis see Fig. S1F.
O: *In-situ* hybridization of embryos at different developmental stages of WT, E(z)-TS (shifted to a permissive temperature at ZGA) and E(z)-KD embryos. The expression boundaries at stage 5 of both *Abd-B* and *Ubx* are established in the same way as in WT embryos (arrowheads). After germband extension at around stage 10 a clear spreading of *Ubx* and *Abd-B* can be observed (arrowheads).
P: DAPI, α-H3K27me3 and α-Abd-B staining of wildtype and E(z)-TS embryos, that were shifted at ZGA to a permissive temperature. The wildtype embryo is at developmental stage 12-13 at which the germband starts retracting. The localization of Abd-B protein is restricted only to the abdominal segments of the embryo (arrowhead). The asterisk marks unspecific staining of the amnioserosa. The E(z)-TS embryo is at developmental stage 9-10, at which the germband is still fully extended. The embryo shows staining of H3K27me3 indicating that E(z) has regained its enzymatic activity after the temperature shift. Still the expression pattern of Abd-B is altered and clearly spreads throughout all segments of the embryo (arrowhead). Scale bar 100 μm. For further details of *Drosophila* embryogenesis see Fig. S1F.
Q: Western blot showing the expression of the maternally and zygotically expressed H3.3 transgenes. The transgenes can be detected through the C-terminal Flag-HA tag. The maternally

deposited H3.3 and H3.3K27M transgenes are detectable before ZGA, while the zygotically expressed transgenes become only detectable in late embryos after ZGA.
For explanation of *Drosophila* embryogenesis see Fig. S1F.

Supplement Figure 3

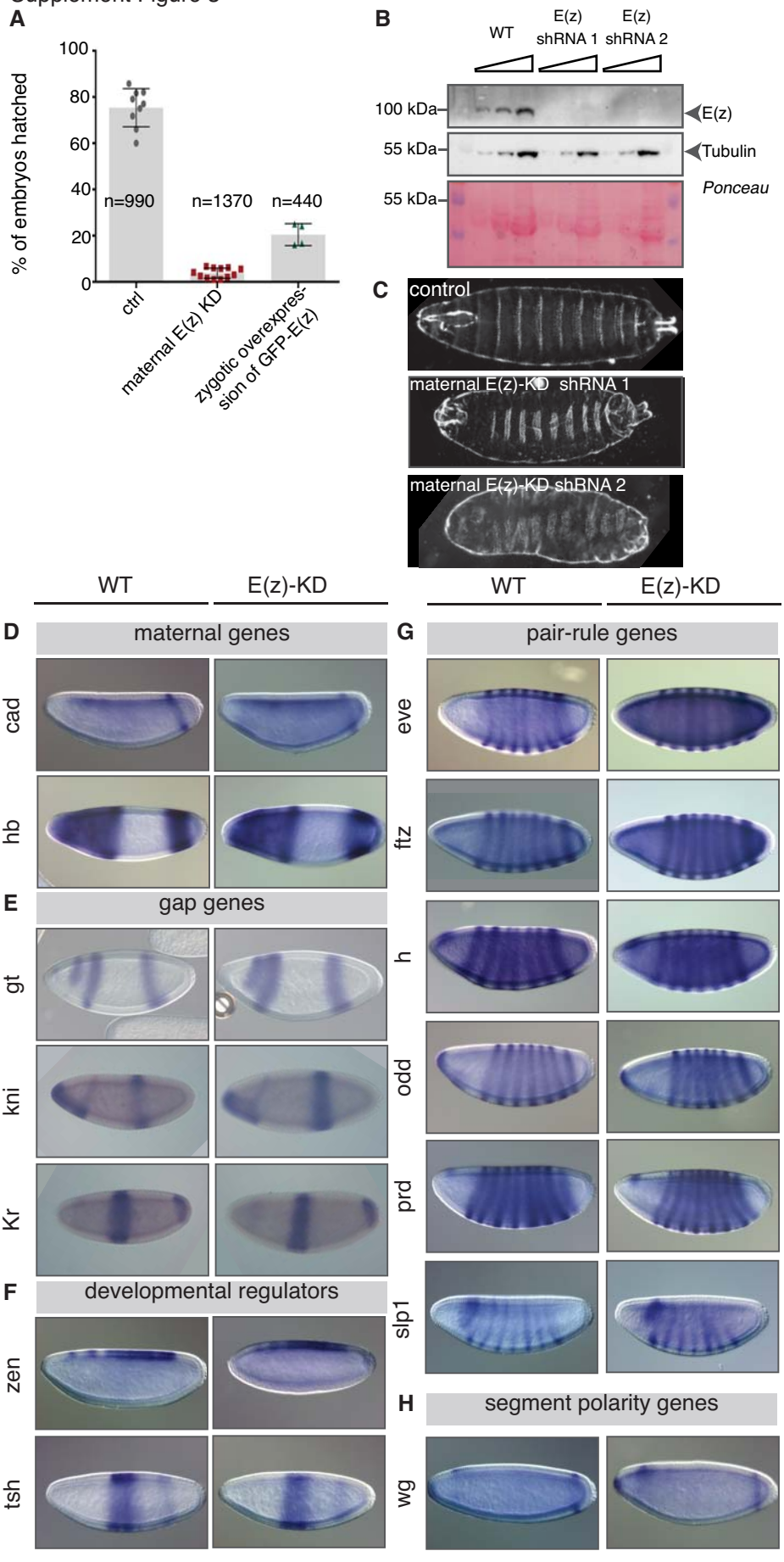

Supplement Figure 3

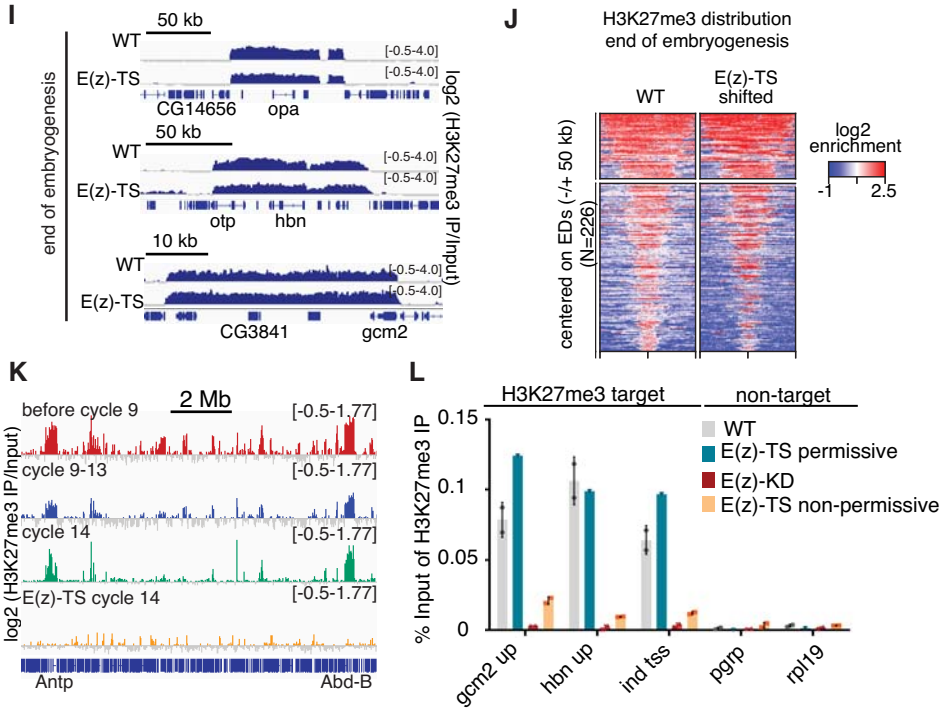

M

		total	classical homeotic	homeotic head	other defect	no cuticle secreted	no pheno-type	not clas-sified
shifted at ZGA	#1	60 (100%)	29 (48%)	13 (22%)	10 (17%)	0 (0%)	3 (5%)	5 (8%)
	#2	39 (100%)	9 (23%)	2 (5%)	14 (36%)	10 (26%)	3 (8%)	1 (3%)
	#3	48 (100%)	15 (31%)	8 (17%)	14 (29%)	6 (13%)	1 (2%)	4 (8%)
	#4	71 (100%)	21 (30%)	10 (14%)	14 (20%)	10 (14%)	2 (3%)	14 (20%)
permis-sive	#1	40 (100%)	2 (5%)	0 (0%)	3 (8%)	0 (0%)	33 (83%)	2 (5%)

Supplement Figure 3

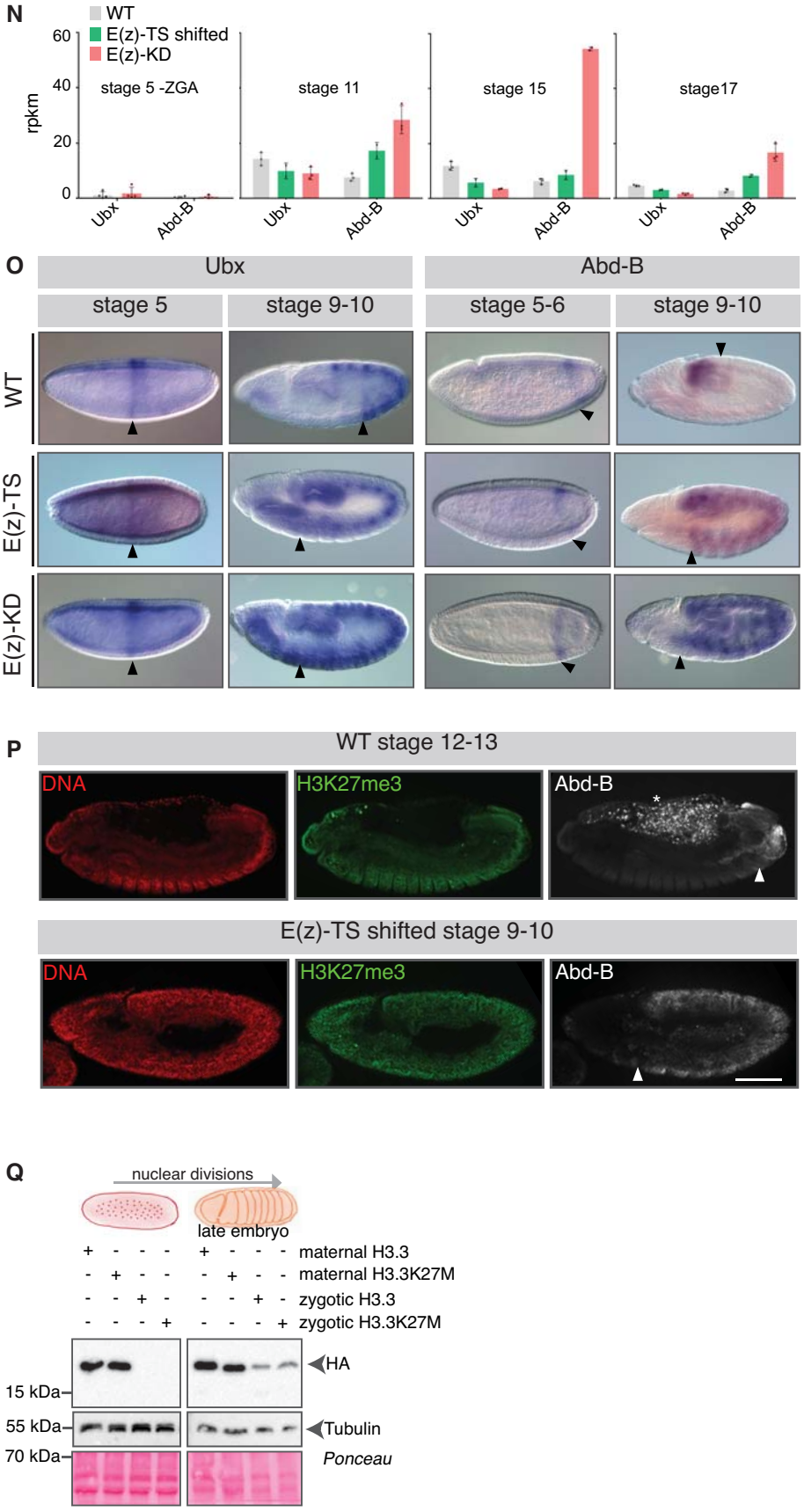

Fig. S4 Early embryonic loss of H3K27me3 leads to increased H3K27ac and transcriptional upregulation of developmental regulator genes

A: Immunofluorescence staining of WT embryos showing the PolII-Ser2-phosphorylated signal on chromatin occurs precisely at ZGA at cycle 14. PolII-Ser2-phosphorylated cannot be detected on the chromatin during earlier mitotic cycles 6-8.

B: Immunofluorescence staining of E(z)-KD embryos showing that the PolII-Ser2-phosphorylated is still detected on the chromatin at ZGA at cycle 14 whereas it cannot be detected on the chromatin during earlier mitotic cycles 6-8. Thus, lack of H3K27me3 does not severely impact the timing of ZGA.

C: Full heat map of H3K27ac (left panel) and H3K4me1 (right panel) ChIP signals in embryos at ZGA showing both replicates. ChIP signals are centered over the union of H3K27ac peaks within 4 kb windows. The heat map on the right depicts the log2 fold changes of H3K27me3 upon E(z)-KD (E(z)-KD/WT). Rows were sorted by differential activity (see Materials and Methods), such that H3K27ac sites within top rows were most strongly elevated in E(z)-KD relative to WT embryos. To test whether the H3K27ac enrichment overlaps with putative enhancer regions the ChIP-signal of H3K4me1 is clustered next to the heatmap. The H3K4me1 profile shows a similar distribution, indicating that the gained H3K27ac peaks fall into enhancer regions. The insets correspond to the sub-clusters shown in Fig. 4A are marked by a grey box. All the peaks and closest gene list is provided in Database S2.

D: The ChIP tracks were generated from embryos at cycle 14. Each example shows H3K4me1 (petrol) in WT embryos, H3K27ac in WT (dark green) and E(z)-KD (light green) embryos and H3K27me3 (blue) in WT embryos. The log2 enrichment of the respective IP over the input is plotted. The RNA-expression track shows the log2FC of the E(z)-KD over the WT (upregulation in the E(z)-KD is shown in red, downregulation in blue). The fifth track in each panel contains the locations of tested enhancers from the Vienna Tiles collection and at the right side of the figure the corresponding LacZ reporter expression patterns in the *Drosophila* embryo. The seventh track shows the top 200 H3K27ac peaks gained upon E(z)-KD (see Fig. 4A). Doc1(*Dorsocross1*) and Doc2 (*Dorsocross2*) are T-box transcription factors. They play important roles in differentiation, cell proliferation arrest and specification of a subset of muscle progenitors.

E: CG13928 has a zinc-finger domain and is expressed in the embryonic nervous system.

F: inaD (*inactivation no afterpotential D*) is a scaffold protein involved in the localization of signaling proteins.

G: Ptx1 is a transcription-factor regulated by a nearby Polycomb Response Element. The regions show strong gain in H3K27ac.

H: Violin plot shows log2 fold expression changes at cycle 9-13 in E(z)-KD vs. WT embryos for the top 200 H3K27ac peak-associated genes (n=155). The top 200 H3K27ac peak-associated genes do not show significant upregulation at this stage and are only significantly upregulated at ZGA (see Fig. 4B)(p=0.1; Wilcoxon test).

I: Meta profiles showing mean read count normalized H3K27ac and H3K27me3 levels centered at the transcription start sites of unique genes (n=155) associated with the top 200 H3K27ac enriched regions in E(z)-KD embryos. The top 200 associated genes are submitted in Database S2.

J: Meta profiles showing mean read count normalized H3K27ac and H3K27me3 levels centered at the transcription start sites of unique genes associated with any H3K27ac site.

K: Enrichment of H3K27me3 in the upstream region of H3K27me3-target and non-target genes in WT and E(z)-KD embryos. E(z)-KD and WT embryos used for qPCR were collected by time 2:20-2:50 h (corresponding to cycle 14) (* individual t-tests $p<0.05$). As negative control the genes *Peptidoglycan recognition protein LE* (*pgrp*) and *Ribosomal protein L19* (*rpl19*) were used. Showing the strong reduction of H3K27me3 upon E(z)-KD.
L: GO analysis of the genes (n=155) associated with the top 200 newly established H3K27ac peaks in E(z)-KD vs. WT embryos.
M: Genome-browser examples of some of the top 200 H3K27ac peaks, that gain H3K27ac at later stages of development in WT embryos. These regions show an accumulation of H3K27ac upon maternal depletion of E(z) in E(z)-KD embryos. The log2 enrichment of the H3K27ac IP over the input is plotted. The H3K27ac ChIP data of WT embryos at late stages was generated in (*23*).
N: Heat map shows H3K27ac enrichment during embryonic development of *Drosophila.* The sorting of the rows corresponds to Fig. S4C. The ChIP signal is centered over the union of H3K27ac peaks within a 4 kb window. A class of peaks that are gained in the E(z)-KD embryos at ZGA appear only at later stages of embryonic development in WT embryos. The ChIP data of later embryonic stages (post-ZGA, gastrulation, all datasets of late embryogenesis) was obtained from modEncode (generated by K. White). For more details see Database S4.
To compare the increase in H3K27ac the p-value of the H3K27ac signal on the top200 peaks was calculated (WT ZGA vs. E(z)-KD ZGA $p=2.2e^{-34}$, WT ZGA vs. WT post-ZGA $p=1.6e^{-20}$, WT ZGA vs. WT gastrulation $p=9.2e^{-20}$, WT ZGA vs. WT late embryogenesis in order of the heat map $p=8.2e^{-16}$, $p=3.8e^{-04}$, $p=0.08$, $p=0.9$, paired Wilcoxon-test).
O: Heat map shows row standardized expression of top 200 H3K27ac-associated genes (Fig. 4A, Database S2) across different stages of *Drosophila* development. K means clustering (n=5) was used to identify groups of genes with similar expression patterns. Most of the top200 associated genes are not expressed at the earliest time point of embryogenesis (early embryo) and become expressed at later stages of development. The expression data was obtained from (*56*) and made available through (*57*).

Supplement Figure 4

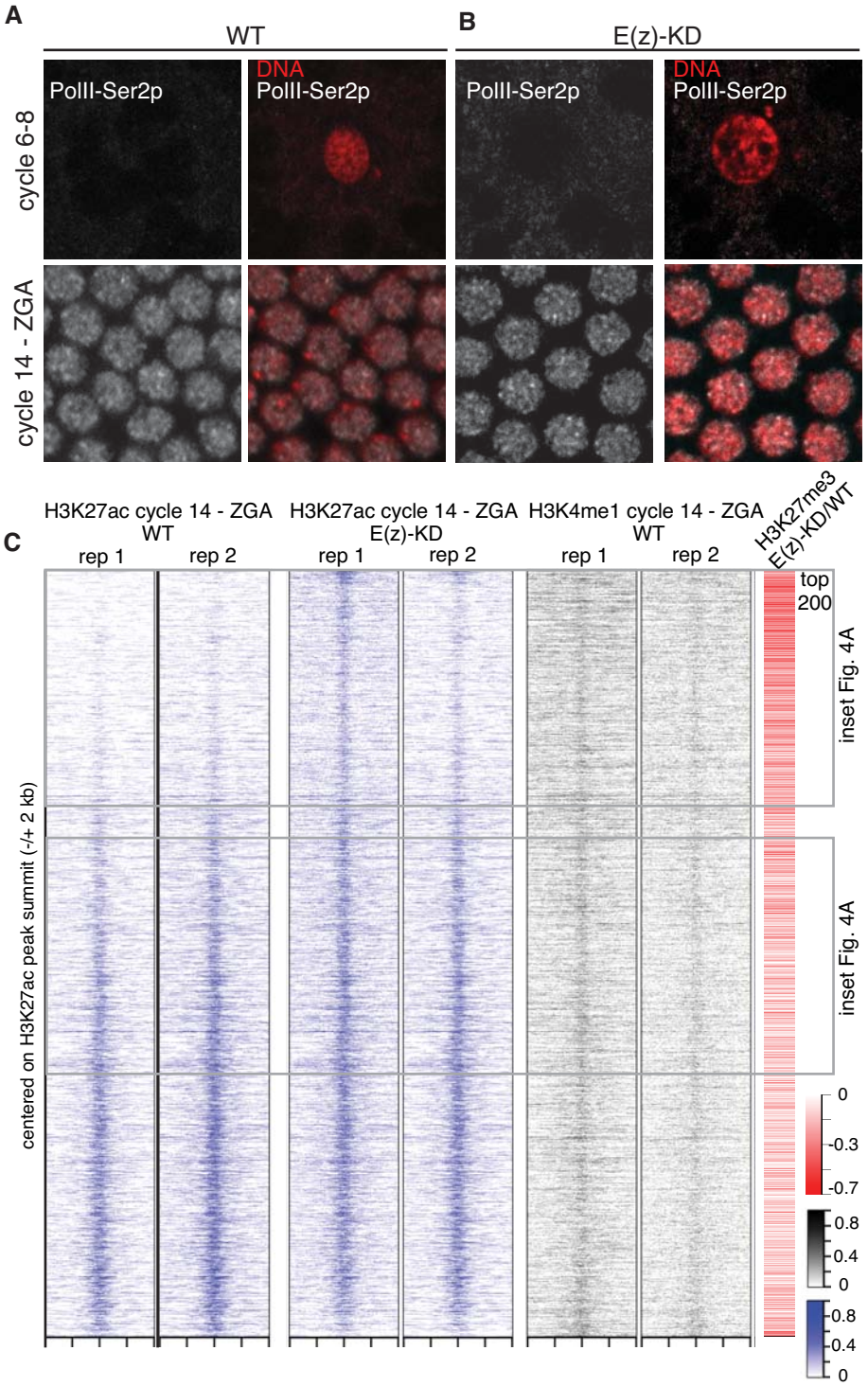

Supplement Figure 4

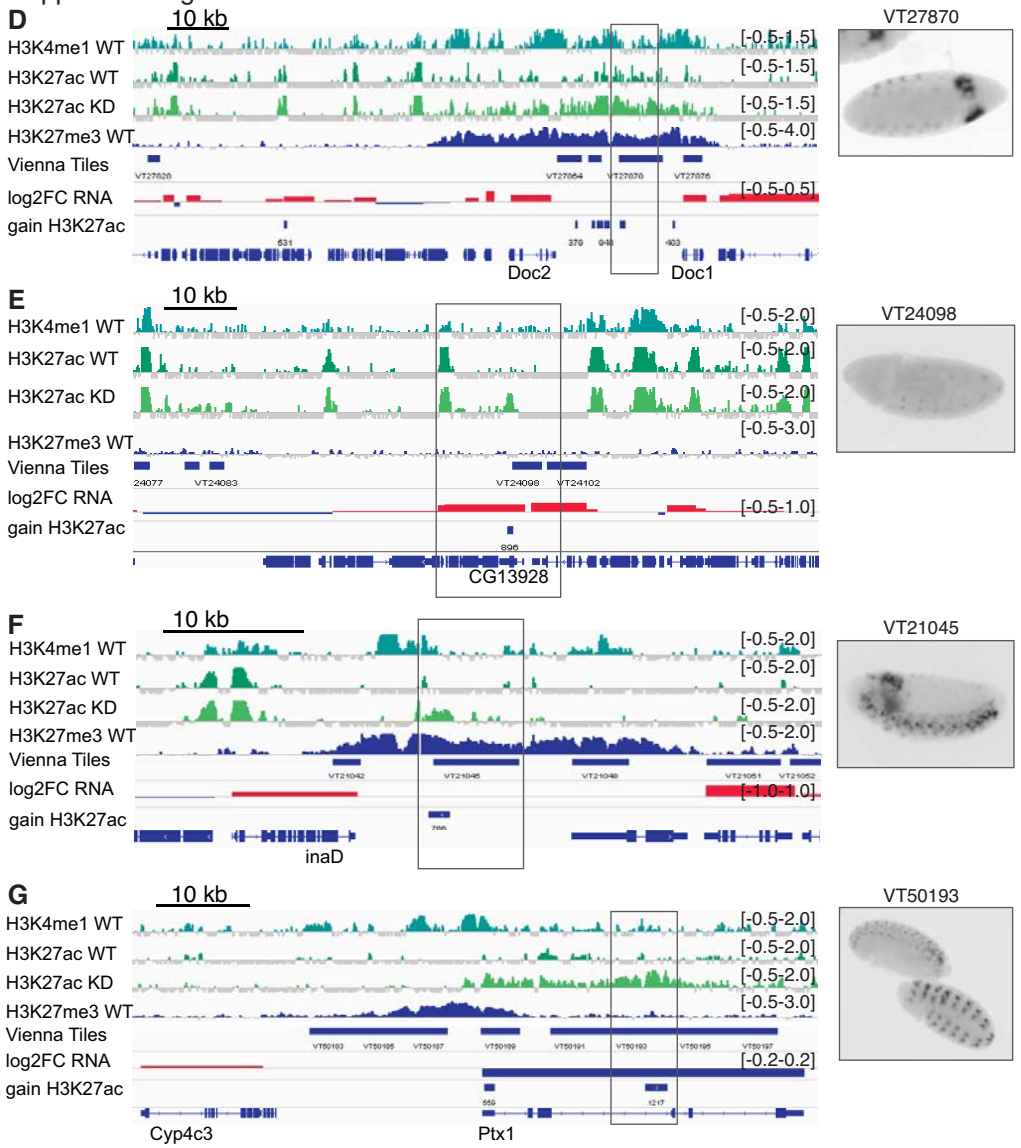

Supplement Figure 4

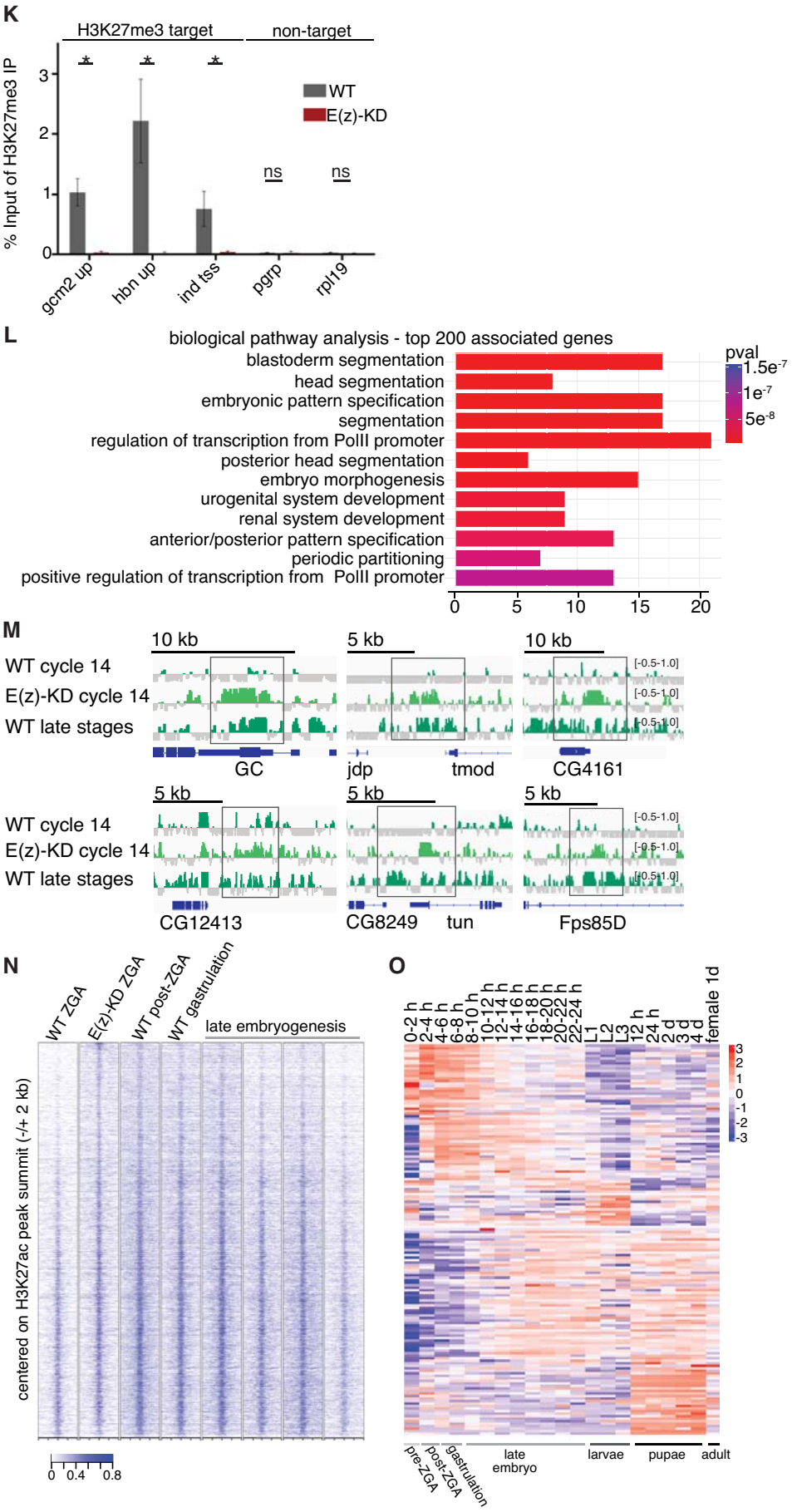

Fig.S5 Spreading of H3K27ac on the Abd-B locus at ZGA leads to misexpression later in development and cannot be reverted by re-establishing H3K27me3 domains.

A: Genome browser snapshot showing the H3K27me3 (blue) and H3K27ac (green) signal (log2 ratio over the input) on the HOX-cluster at zygotic genome activation and in late embryogenesis. Already at ZGA the H3K27ac signal spreads into *Abd-B* genomic region upon E(z)-KD. The spreading of H3K27ac into *Abd-B* genomic region is still detectable at stage 17 in E(z)-KD and in embryos of the E(z)-TS that were shifted at ZGA to a permissive temperature. The WT H3K27me3 and H3K27ac track of late embryos was retrieved from GEO and has been mapped and analyzed using the same pipeline as for the data generated in this study (for further details see Database S4-3) (*23, 58*).

Supplement Figure 5

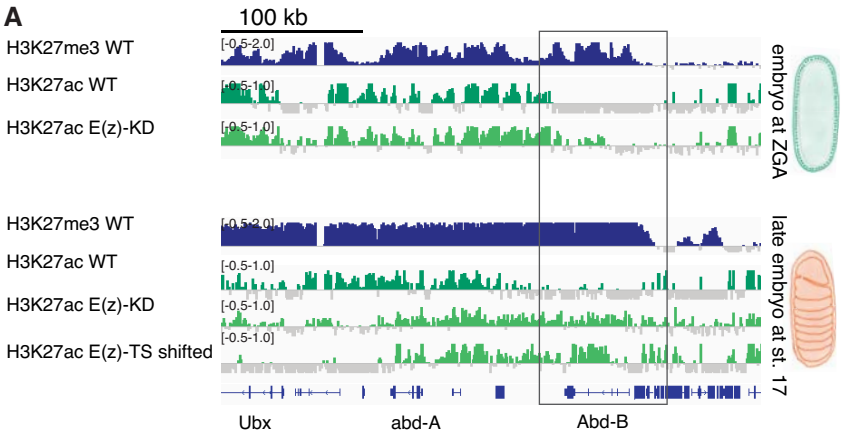

Table S1 Fly lines

Description of all fly lines used in this study.

BDSC	Transgene/allele	referred to as	Source	Experiment	reference
33659	V20 RNAi E(z) attP2	E(z)-KD shRNA2	BDSC	RNAi KD of E(z)	
36303	attP2 integration site		BDSC	control for RNAi KD	
7063	matα4-GAL-VP16		BDSC	driverline to induce late oogenesis RNAi (~st. 3-4)	
	E(z)>HA:E(z) Transgene at 51C locus - 2R	HA-E(z)	gift of V. Pirrotta	expression of HA-E(z) under its endogenous promoter	unpublished
	E(z)>HA:E(z) Transgene at 51C locus - 2R/V20 RNAi E(z) attP2			co-expression E(z)-RNAi and E(z)>HA:E(z)	unpublished
	tubulin>GFP:E(z)		gift of L. Ringrose	overexexpression of GFP-E(z) under tubulin promoter	(*40*)
	E(z)61 (C603Y)	E(z)-TS	gift of V. Pirrotta	maternal/zygotic depletion of E(z)'s enzymatic function	(*59*) (*17*)
58410	w*; PBac(UAS-H3.3.FLAG.HA)/ CyO;	zygotic H3.3	BDSC	zygotic overexpression of H3.3 and the mutant version K27M	(*28*)
58412	w*; PBac(UAS-H3.3.K27M.FLAG.HA)/ CyO;	zygotic H3.3 K27M	BDSC	zygotic overexpression of H3.3 and the mutant version K27M	
	V20 RNAi E(z) attP40	E(z)-KD shRNA1	generated in this study	RNAi KD of E(z)	See Table S3 and Cloning and generation of transgenic flies
	w; pUASp-attB dmel/H3.3::Flag-HA/ CyO;	maternal H3.3	generated in this study	maternal overexpression of H3.3 and the mutant version K27M	See Table S3 and Cloning and generation of transgenic flies
	w; pUASp-attB dmel/H3.3 K27M::Flag-HA/CyO	maternal H3.3 K27M	generated in this study	maternal overexpression of H3.3 and the mutant version K27M	See Table S3 and Cloning and generation of transgenic flies
9752	y[1] w[1118]; PBac(y[+]-attP-3B)VK00037		BDSC	attP line to generate maternal H3.3 overexpression lines	
25709	y[1] v[1] P(y[+t7.7]=nos-phiC31\int.NLS)X; P(y[+t7.7]=CaryP)attP40		BDSC	attP line to generate E(z)-KD shRNA1 line	

Table S2 Antibodies

Description of all antibodies used in this study.

Antigen	host species	Manufacturer, catalogue number	Lot-Nr.	Experiment	dilution
H3K27me3	rabbit	Diagenode, C15410195	A1811-001P	ChIP	1 µg
H3K27me3	rabbit	Thomas Jenuwein Lab		IF	1:100-1:200
H3K27me3	rabbit	Thomas Jenuwein Lab		Western Blot	1:1000
H3K27me3	rabbit	Thomas Jenuwein Lab		ChiP	1:2000
H3K27me3	rabbit	Millipore, 07-449	JBC1858854	IF	1:100
H3K27me3	rabbit	Millipore, 07-449	JBC1858854	ChIP	1 µg
H3K27me3	mouse	abcam, ab6002	554383	Western Blot	1:1000
H3K27me3	mouse	Diagenode C15200181-50		IF	1:100
H3K27me2	rabbit	Thomas Jenuwein Lab		Western Blot	1:1000
H3K4me1	rabbit	Diagenode, C15410194	A1862D	ChIP	1 µg
H3K4me1	rabbit	Active Motif, 39297, 39298		IF	1:100
H3K27ac	rabbit	Diagenode, C15410196	A1723-041D	ChIP	1 µg
H3K27ac	mouse	GeneTex, GTX50903		IF	1:100
H3K4me3	rabbit	Diagenode, C15410003		IF	1:100
H3	rabbit	abcam, ab1791		Western Blot	1:3000-1:30000
PolII-Ser2-phosphorylated	rabbit	abcam, ab5095		IF	1:100
HA.11	mouse	Covance 16B12	MMS101R	IF	1:200
Tubulin	mouse	Sigma DM1	T9026	Western Blot	1:3000
E(z)	rabbit	Juerg Mueller		Western Blot	1:1000
Abd-B	mouse	DSHB, 1A2E9		IF	1:20
Alexa-Fluor conjugated antibodies		MolecularProbes, ThermoScientific		IF	1:500
HRP conjugated antibodies		Jackson ImmunoResearch		Western Blot	1:5000
AP-conjugated DIG antibody		Roche 11093274910		in situ	1:500

Table S3 Primer

Description of all primers used in this study.

Sequence	Name	Tm	Experiment	
ACATGCTGCCCACCGGATTCA	o53 Rp49_Fw :	58	mRNA expression	
CAATCTCCTTGCGCTTCTTGGA	o54 Rp49_Rv :	58	mRNA expression	
CTAAGCTGTCGCACAAATGG	o111 5'RT-RP49_pair2	60	mRNA expression	
GGGCATCAGATACTGTCCCT	o112 3'RT-RP49_pair2	59	mRNA expression	
ATGCCAGCCATAATGGAGTT	o13 5'RT-E(z)-pair3	59	mRNA expression	
GCAAGGATAATGGCCTGACT	o14 3'RT-E(z)-pair3	59	mRNA expression	
AATCATCATCGGGTTTCTGGAGG	o181 GluRIIA_qPCR_2fw	62	mRNA expression	DRSC
CGCCATTGGAAATCAGTTCACA	o182 GluRIIA_qPCR_2rev	61	mRNA expression	
ATACCCCAAAGCGATGTCGAG	o189 Sry-delta_qPCR_2fw	62	mRNA expression	DRSC
ACGAACTCTCTCTTTATCTCCGT	o190 Sry-delta_qPCR_2rev	60	mRNA expression	
TGCCACACCATCTCAGCTAC	o193 CG14013_qPCR_2fw	60	mRNA expression	
CGATGCATGAACATCAGTCC	o194 CG14013_qPCR_2rev	60	mRNA expression	
TATGTCTATCGCAGGACTAACGG	o183_Prosalpha6T_qPCR_1fw	61	mRNA expression	DRSC
CAGCTTGTTACCCAGATTGGAAA	o184_Prosalpha6T_qPCR_1rev	60.7	mRNA expression	
GCCAACCAGACATACTGCG	o367_ncd_qPCR_1fw	61	mRNA expression	DRSC
CTACGGCTACGTCTCAGCTTG	o368_ncd_qPCR_1rev	62	mRNA expression	
ATGGAAACGCAACCTGAGGTG	o505_taf2_qPCR_1_fw	62	mRNA expression	DRSC
CACGCCGATTATGCTCCTCC	o506_taf2_qPCR_1_rev	62	mRNA expression	
ATGGCTGCACACAAGTCGTT	o511_rpl39_qPCR_2_fw	62	mRNA expression	DRSC
TAGGCGAACCCATTGGGGA	o512_rpl39_qPCR_2_rev	62	mRNA expression	
TGAGCTTTCCAACACTCTTGC	o75 PGRP-TSS-Fw	54	ChIP-qPCR	
GGTTTTGGTGGTTTATCTGAG	o76 PGRP-TSS-Rev	50	ChIP-qPCR	
CTGTCCATCTCCGATGACCT	o241 sry-d_12kb_up_1_fw (K27m3)	60	ChIP-qPCR	
GATCTCGGGATTCGTCTTGA	o242 sry-d_12kb_up_1_rev (K27m3)	60	ChIP-qPCR	
TTCAGAATGCACTTCAACCG	o245 GluRIIA_2kb_up_peak_fw	60	ChIP-qPCR	
TCAGTCAGTCTGGCGATTGT	o246 GluRIIA_2kb_up_peak_rev	60	ChIP-qPCR	
GAAATTTGCGCCATAGGAAG	o263 prosalpha6T_2kb_up_1_fw	60	ChIP-qPCR	
CTGTGCGCGAGCAGTTAAT	o264 prosalpha6T_2kb_up_1_rev	60	ChIP-qPCR	
atgcgcctatcagcttgtg	FZ011_RpL19-TSS_fw	55	ChIP-qPCR	(*60*)
gacaagtgccattctgtttcc	FZ012_RpL19-TSS_rev	50	ChIP-qPCR	(*60*)
catcttgggtttctggggta	FZ015_ind-TSS_fw	50	ChIP-qPCR	(*60*)
gacagtttcgcacagtcagc	FZ016_ind-TSS_rev	55	ChIP-qPCR	(*60*)
atgatcgtgggagtttctcg	FZ017_gcm2-up_fw	52	ChIP-qPCR	(*60*)
tgctcagcattctgttttgg	FZ018_gcm2-up_rev	52	ChIP-qPCR	(*60*)
tgtggcaattctctctggtg	FZ019_hbn-up_fw	52	ChIP-qPCR	(*60*)
tgtttgtgggttgttgtcgt	FZ020_hbn-up_rev	50	ChIP-qPCR	(*60*)
caccATGGCACGTACCAAGCAAACAGCC	FZ80_cacc_H3.3A_fw	60	H3.3-FLAG-HA	
GCGGCCCGTAtgTCGGCGCCATC	FZ81_H3.3A_K27M_fw	65	H3.3-FLAG-HA	
GATGGCGCCGAcaTACGGGCCGC	FZ82_H3.3A_K27M_rev	65	H3.3-FLAG-HA	

CTAGGCGTAGTCGGGCACGTCGTAGGGGTATCCTCCAGCGGCCGACTTGTCATCGTCATCCTTGTAATCTCCTCCAGCGGCCGCGGCCCGCTCGCCACGGATGCG	FZ83_H3.3A_FLAG-HA_rev	65	H3.3-FLAG-HA	
ACTAGTATGGCACGTACCAAGCAAACAGCC	VA01_SpeI_H3.3_fw	60	H3.3-FLAG-HA	
GGATCCCTAGGCGTAGTCGGGCACGTCG	VA02_HA_BamHI_rev	62	H3.3-FLAG-HA	
ctagcagtGTATCATACAAATTGAATAAAtagttatattcaagcataTTTATTCAATTTGTATGATACgcg	FZ028 shRNA 3UTR e(z) topstrand	-	RNAi	
aattcgcGTATCATACAAATTGAATAAAtatgcttgaatataactaTTTATTCAATTTGTATGATACactg	FZ029 shRNA 3UTR e(z) bottomstrand	-	RNAi	
TCTAGATAATACGACTCACTATAGGGATGCACGGATACCGAACCTAC	FZ103_XbaI_T7_eve_fw	53	probe	
tctagaAATTAACCCTCACTAAAGGGTTACGCCTCAGTCTTGTAGGG	FZ104_eve_T3_XbaI_rev	54	probe	
TCTAGATAATACGACTCACTATAGGGATGGCCACCACAAACAGCCAG	FZ105_XbaI_T7_ftz_fw	56	probe	
tctagaAATTAACCCTCACTAAAGGGTCAAGACAGATGGTAGAGGTCCTG	FZ106_ftz_T3_XbaI_rev	56	probe	
TCTAGATAATACGACTCACTATAGGGATGTTACACGAGGCTCTGATGC	FZ107_XbaI_T7_tsh_fw	56	probe	
tctagaAATTAACCCTCACTAAAGGGTTAGGCGGTCTTCTCCTTCTTC	FZ108_tsh_T3_XbaI_rev	55	probe	
TCTAGATAATACGACTCACTATAGGGATGGTTTCGCACTACTACAACACAC	FZ109_XbaI_T7_cad_fw	56	probe	
tctagaAATTAACCCTCACTAAAGGGTCACATCGAGAGCGTGCCC	FZ110_cad_T3_XbaI_rev	56	probe	
TCTAGATAATACGACTCACTATAGGGATGACCGTAACCGCCTTTGC	FZ111_XbaI_T7_prd_fw	55	probe	
tctagaAATTAACCCTCACTAAAGGGCTAGTACCATGAGGGATAGAACG	FZ112_prd_T3_XbaI_rev	54	probe	
TCTAGATAATACGACTCACTATAGGGATGTCTTCCACATCGGCCTC	FZ113_XbaI_T7_odd_fw	54	probe	
tctagaAATTAACCCTCACTAAAGGGCTATCTGCTCATGATCTCATCG	FZ114_odd_T3_XbaI_rev	54	probe	
tctagaTAATACGACTCACTATAGGGATGGTGAAAAGTGAAATGGAATTC	FZ117_XbaI_T7_slp1_fw	50	probe	
tctagaAATTAACCCTCACTAAAGGGTTAGCTGGATGGAAACTTGCC	FZ118_slp1_T3_XbaI_rev	52	probe	
tctagaTAATACGACTCACTATAGGGATGCAGAACTGGGAGACGAC	FZ121_XbaI_T7_hb_fw	53	probe	
tctagaAATTAACCCTCACTAAAGGGTTAGGAGTGAGCATTCCTGGC	FZ122_hb_T3_XbaI_rev	54	probe	
tctagaTAATACGACTCACTATAGGGATGGTTACCGGCGTAACAGCAGCC	FZ123_XbaI_T7_h_fw	60	probe	
tctagaAATTAACCCTCACTAAAGGGCTACCAGGGCCGCCAGGGC	FZ124_h_T3_XbaI_rev	60	probe	
tctagaTAATACGACTCACTATAGGGATGTCATCCGTCATGCACTAC	FZ125_XbaI_T7_zen_fw	52	probe	
tctagaAATTAACCCTCACTAAAGGGTTAGTTGGGATAATTGTAGGAGG	FZ126_zen_T3_XbaI_rev	52	probe	
tctagaTAATACGACTCACTATAGGGATGGATATCAGCTATATCTTCGTC	FZ135_XbaI_T7_wg_fw	52	probe	
tctagaAATTAACCCTCACTAAAGGGTTACAGACACGTGTAGATGACC	FZ136_wg_T3_XbaI_rev	53	probe	
tctagaAATTAACCCTCACTAAAGGGTCACTGGTGCATCTTGGCGGCATG	FZ172_abd-B_RB_CDS_XbaI_T3_rev	60	probe	
tctagaTAATACGACTCACTATAGGGATGTCCATACAATTAGCGCCACTGC	FZ172_XbaI_T7_abd-B_RJ_CDS_fw	60	probe	
tctagaTAATACGACTCACTATAGGGATGAACTCGTACTTTGAACAGGCC	FZ129_XbaI_T7_ubx_fw	55	probe	
tctagaAATTAACCCTCACTAAAGGGCTACTGATCTAAGTGTCCACC	FZ130_ubx_T3_XbaI_rev	52	probe	

Additional Databases S1-S4 (files in zipped archives)

Databases S1 to S4 as zipped archives

Additional Database S1: 1 ED annotation
1-H3K27me3_bef_C9_EDs.bed
2-H3K27me3_C9_C13_EDs.bed
3-H3K27me3_C14_EDs.bed
4-EDs_merged.bed
5- H3K27me3_EzTS_shifted_st17_EDs
6- H3K27me3_WT_16-18h_EDs
7- Number_of_EDs_development

Additional Database S2: 2 Top200 annotation
1-H3K27ac_peak_anno_stage5_new_gene_list.tsv
2-Top200_associated_genes.txt

Additional Database S3: 3 DESeq
1- DESeq2_out_cycle9_13.tsv
2- DESeq2_out_stage5.tsv

Additional Database S4: 4 generated datasets
1-NGS_overview_samples_ChIP
2-NGS_overview_samples_RNA
3-Public_datasets

References

1. H. D. Morgan, F. Santos, K. Green, W. Dean, W. Reik, Epigenetic reprogramming in mammals. *Hum. Mol. Genet.* **14** (suppl. 1), R47–R58 (2005). doi:10.1093/hmg/ddi114 Medline

2. E. A. Miska, A. C. Ferguson-Smith, Transgenerational inheritance: Models and mechanisms of non-DNA sequence-based inheritance. *Science* **354**, 59–63 (2016). doi:10.1126/science.aaf4945 Medline

3. U. Sharma, O. J. Rando, Metabolic inputs into the epigenome. *Cell Metab.* **25**, 544–558 (2017). doi:10.1016/j.cmet.2017.02.003 Medline

4. J. A. Simon, R. E. Kingston, Mechanisms of polycomb gene silencing: Knowns and unknowns. *Nat. Rev. Mol. Cell Biol.* **10**, 697–708 (2009). Medline

5. U. Grossniklaus, R. Paro, Transcriptional silencing by polycomb-group proteins. *Cold Spring Harb. Perspect. Biol.* **6**, a019331 (2014). doi:10.1101/cshperspect.a019331 Medline

6. N. Iovino, F. Ciabrelli, G. Cavalli, PRC2 controls *Drosophila* oocyte cell fate by repressing cell cycle genes. *Dev. Cell* **26**, 431–439 (2013). doi:10.1016/j.devcel.2013.06.021 Medline

7. W. Mu, J. Starmer, A. M. Fedoriw, D. Yee, T. Magnuson, Repression of the soma-specific transcriptome by Polycomb-repressive complex 2 promotes male germ cell development. *Genes Dev.* **28**, 2056–2069 (2014). doi:10.1101/gad.246124.114 Medline

8. U. Brykczynska, M. Hisano, S. Erkek, L. Ramos, E. J. Oakeley, T. C. Roloff, C. Beisel, D. Schübeler, M. B. Stadler, A. H. F. M. Peters, Repressive and active histone methylation mark distinct promoters in human and mouse spermatozoa. *Nat. Struct. Mol. Biol.* **17**, 679–687 (2010). doi:10.1038/nsmb.1821 Medline

9. S. Hontelez, I. van Kruijsbergen, G. Georgiou, S. J. van Heeringen, O. Bogdanovic, R. Lister, G. J. C. Veenstra, Embryonic transcription is controlled by maternally defined chromatin state. *Nat. Commun.* **6**, 10148 (2015). doi:10.1038/ncomms10148 Medline

10. S. S. Hammoud, D. A. Nix, H. Zhang, J. Purwar, D. T. Carrell, B. R. Cairns, Distinctive chromatin in human sperm packages genes for embryo development. *Nature* **460**, 473–478 (2009). Medline

11. X. Y. Li, M. M. Harrison, J. E. Villalta, T. Kaplan, M. B. Eisen, Establishment of regions of genomic activity during the *Drosophila* maternal to zygotic transition. *eLife* **3**, 03737 (2014). doi:10.7554/eLife.03737 Medline

12. N. L. Vastenhouw, Y. Zhang, I. G. Woods, F. Imam, A. Regev, X. S. Liu, J. Rinn, A. F. Schier, Chromatin signature of embryonic pluripotency is established during genome activation. *Nature* **464**, 922–926 (2010). doi:10.1038/nature08866 Medline

13. H. Zheng, B. Huang, B. Zhang, Y. Xiang, Z. Du, Q. Xu, Y. Li, Q. Wang, J. Ma, X. Peng, F. Xu, W. Xie, Resetting epigenetic memory by reprogramming of histone modifications in mammals. *Mol. Cell* **63**, 1066–1079 (2016). doi:10.1016/j.molcel.2016.08.032 Medline

14. L. J. Gaydos, W. Wang, S. Strome, H3K27me and PRC2 transmit a memory of repression across generations and during development. *Science* **345**, 1515–1518 (2014). doi:10.1126/science.1255023 Medline

15. M. Samson, M. M. Jow, C. C. L. Wong, C. Fitzpatrick, A. Aslanian, I. Saucedo, R. Estrada, T. Ito, S. K. Park, J. R. Yates 3rd, D. S. Chu, The specification and global reprogramming of histone epigenetic marks during gamete formation and early embryo development in *C. elegans*. *PLOS Genet.* **10**, e1004588 (2014). doi:10.1371/journal.pgen.1004588 Medline

16. G. Struhl, D. Brower, Early role of the *esc*$^{+}$ gene product in the determination of segments in *Drosophila*. *Cell* **31**, 285–292 (1982). doi:10.1016/0092-8674(82)90428-7 Medline

17. R. S. Jones, W. M. Gelbart, Genetic analysis of the enhancer of zeste locus and its role in gene regulation in *Drosophila melanogaster*. *Genetics* **126**, 185–199 (1990). Medline

18. A. H. Elnfati, D. Iles, D. Miller, Nucleosomal chromatin in the mature sperm of *Drosophila melanogaster*. *Genom. Data* **7**, 175–177 (2015). doi:10.1016/j.gdata.2015.12.021 Medline

19. S. F. Wu, H. Zhang, B. R. Cairns, Genes for embryo development are packaged in blocks of multivalent chromatin in zebrafish sperm. *Genome Res.* **21**, 578–589 (2011). doi:10.1101/gr.113167.110 Medline

20. T. Cheutin, G. Cavalli, Progressive polycomb assembly on H3K27me3 compartments generates polycomb bodies with developmentally regulated motion. *PLOS Genet.* **8**, e1002465 (2012). doi:10.1371/journal.pgen.1002465 Medline

21. A. J. Haigh, W. A. MacDonald, V. K. Lloyd, The generation of cloned *Drosophila melanogaster*. *Genetics* **169**, 1165–1167 (2005). doi:10.1534/genetics.104.035113 Medline

22. W. Tadros, H. D. Lipshitz, The maternal-to-zygotic transition: A play in two acts. *Development* **136**, 3033–3042 (2009). doi:10.1242/dev.033183 Medline

23. S. K. Bowman, A. M. Deaton, H. Domingues, P. I. Wang, R. I. Sadreyev, R. E. Kingston, W. Bender, H3K27 modifications define segmental regulatory domains in the *Drosophila* bithorax complex. *eLife* **3**, e02833 (2014). doi:10.7554/eLife.02833 Medline

24. M. D. Schroeder, C. Greer, U. Gaul, How to make stripes: Deciphering the transition from non-periodic to periodic patterns in *Drosophila* segmentation. *Development* **138**, 3067–3078 (2011). doi:10.1242/dev.062141 Medline

25. F. Pelegri, R. Lehmann, A role of polycomb group genes in the regulation of gap gene expression in *Drosophila*. *Genetics* **136**, 1341–1353 (1994). Medline

26. Ö. Copur, J. Müller, The histone H3-K27 demethylase Utx regulates HOX gene expression in *Drosophila* in a temporally restricted manner. *Development* **140**, 3478–3485 (2013). doi:10.1242/dev.097204 Medline

27. R. Margueron, N. Justin, K. Ohno, M. L. Sharpe, J. Son, W. J. Drury 3rd, P. Voigt, S. R. Martin, W. R. Taylor, V. De Marco, V. Pirrotta, D. Reinberg, S. J. Gamblin, Role of the polycomb protein EED in the propagation of repressive histone marks. *Nature* **461**, 762–767 (2009). doi:10.1038/nature08398 Medline

28. H. M. Herz, M. Morgan, X. Gao, J. Jackson, R. Rickels, S. K. Swanson, L. Florens, M. P. Washburn, J. C. Eissenberg, A. Shilatifard, Histone H3 lysine-to-methionine mutants as a paradigm to study chromatin signaling. *Science* **345**, 1065–1070 (2014). doi:10.1126/science.1255104 Medline

29. A. Rada-Iglesias, R. Bajpai, T. Swigut, S. A. Brugmann, R. A. Flynn, J. Wysocka, A unique chromatin signature uncovers early developmental enhancers in humans. *Nature* **470**, 279–283 (2011). doi:10.1038/nature09692 Medline

30. S. Bonn, R. P. Zinzen, C. Girardot, E. H. Gustafson, A. Perez-Gonzalez, N. Delhomme, Y. Ghavi-Helm, B. Wilczyński, A. Riddell, E. E. M. Furlong, Tissue-specific analysis of chromatin state identifies temporal signatures of enhancer activity during embryonic development. *Nat. Genet.* **44**, 148–156 (2012). doi:10.1038/ng.1064 Medline

31. E. Z. Kvon, T. Kazmar, G. Stampfel, J. O. Yáñez-Cuna, M. Pagani, K. Schernhuber, B. J. Dickson, A. Stark, Genome-scale functional characterization of *Drosophila* developmental enhancers in vivo. *Nature* **512**, 91–95 (2014). Medline

32. J. L. Haynie, The maternal and zygotic roles of the gene Polycomb in embryonic determination in *Drosophila melanogaster*. *Dev. Biol.* **100**, 399–411 (1983). doi:10.1016/0012-1606(83)90234-8 Medline

33. N. J. Francis, N. E. Follmer, M. D. Simon, G. Aghia, J. D. Butler, Polycomb proteins remain bound to chromatin and DNA during DNA replication in vitro. *Cell* **137**, 110–122 (2009). doi:10.1016/j.cell.2009.02.017 Medline

34. N. Soshnikova, D. Duboule, Epigenetic temporal control of mouse *Hox* genes in vivo. *Science* **324**, 1320–1323 (2009). doi:10.1126/science.1171468 Medline

35. X. Liu, C. Wang, W. Liu, J. Li, C. Li, X. Kou, J. Chen, Y. Zhao, H. Gao, H. Wang, Y. Zhang, Y. Gao, S. Gao, Distinct features of H3K4me3 and H3K27me3 chromatin domains in pre-implantation embryos. *Nature* **537**, 558–562 (2016). doi:10.1038/nature19362 Medline

36. J. Schindelin, I. Arganda-Carreras, E. Frise, V. Kaynig, M. Longair, T. Pietzsch, S. Preibisch, C. Rueden, S. Saalfeld, B. Schmid, J.-Y. Tinevez, D. J. White, V. Hartenstein, K. Eliceiri, P. Tomancak, A. Cardona, Fiji: An open-source platform for biological-image analysis. *Nat. Methods* **9**, 676–682 (2012). doi:10.1038/nmeth.2019 Medline

37. S. Takeo, S. K. Swanson, K. Nandanan, Y. Nakai, T. Aigaki, M. P. Washburn, L. Florens, R. S. Hawley, Shaggy/glycogen synthase kinase 3β and phosphorylation of Sarah/regulator of calcineurin are essential for completion of *Drosophila* female meiosis. *Proc. Natl. Acad. Sci. U.S.A.* **109**, 6382–6389 (2012). doi:10.1073/pnas.1120367109 Medline

38. K. Chang, K. Marran, A. Valentine, G. J. Hannon, Generation of transgenic *Drosophila* expressing shRNAs in the miR-1 backbone. *Cold Spring Harb. Protoc.* **2014**, pdb.prot080762 (2014). doi:10.1101/pdb.prot080762 Medline

39. J. Q. Ni, R. Zhou, B. Czech, L.-P. Liu, L. Holderbaum, D. Yang-Zhou, H.-S. Shim, R. Tao, D. Handler, P. Karpowicz, R. Binari, M. Booker, J. Brennecke, L. A. Perkins, G. J. Hannon, N. Perrimon, A genome-scale shRNA resource for transgenic RNAi in *Drosophila*. *Nat. Methods* **8**, 405–407 (2011). doi:10.1038/nmeth.1592 Medline

40. P. A. Steffen, J. P. Fonseca, C. Gänger, E. Dworschak, T. Kockmann, C. Beisel, L. Ringrose, Quantitative in vivo analysis of chromatin binding of Polycomb and Trithorax group proteins reveals retention of ASH1 on mitotic chromatin. *Nucleic Acids Res.* **41**, 5235–5250 (2013). doi:10.1093/nar/gkt217 Medline

41. B. Langmead, S. L. Salzberg, Fast gapped-read alignment with Bowtie 2. *Nat. Methods* **9**, 357–359 (2012). doi:10.1038/nmeth.1923 Medline

42. H. Li, B. Handsaker, A. Wysoker, T. Fennell, J. Ruan, N. Homer, G. Marth, G. Abecasis, R. Durbin, The Sequence Alignment/Map format and SAMtools. *Bioinformatics* **25**, 2078–2079 (2009). doi:10.1093/bioinformatics/btp352 Medline

43. Y. Zhang, T. Liu, C. A. Meyer, J. Eeckhoute, D. S. Johnson, B. E. Bernstein, C. Nusbaum, R. M. Myers, M. Brown, W. Li, X. S. Liu, Model-based analysis of ChIP-Seq (MACS). *Genome Biol.* **9**, R137 (2008). doi:10.1186/gb-2008-9-9-r137 Medline

44. R. C. Gentleman, V. J. Carey, D. M. Bates, B. Bolstad, M. Dettling, S. Dudoit, B. Ellis, L. Gautier, Y. Ge, J. Gentry, K. Hornik, T. Hothorn, W. Huber, S. Iacus, R. Irizarry, F. Leisch, C. Li, M. Maechler, A. J. Rossini, G. Sawitzki, C. Smith, G. Smyth, L. Tierney, J. Y. H. Yang, J. Zhang, Bioconductor: Open software development for computational biology and bioinformatics. *Genome Biol.* **5**, R80 (2004). doi:10.1186/gb-2004-5-10-r80 Medline

45. J. Zhu, M. Adli, J. Y. Zou, G. Verstappen, M. Coyne, X. Zhang, T. Durham, M. Miri, V. Deshpande, P. L. De Jager, D. A. Bennett, J. A. Houmard, D. M. Muoio, T. T. Onder, R. Camahort, C. A. Cowan, A. Meissner, C. B. Epstein, N. Shoresh, B. E. Bernstein,

Genome-wide chromatin state transitions associated with developmental and environmental cues. *Cell* **152**, 642–654 (2013). doi:10.1016/j.cell.2012.12.033 Medline

46. A. Akalin, V. Franke, K. Vlahoviček, C. E. Mason, D. Schübeler, Genomation: A toolkit to summarize, annotate and visualize genomic intervals. *Bioinformatics* **31**, 1127–1129 (2015). doi:10.1093/bioinformatics/btu775 Medline

47. G. Yu, L. G. Wang, Q. Y. He, ChIPseeker: An R/Bioconductor package for ChIP peak annotation, comparison and visualization. *Bioinformatics* **31**, 2382–2383 (2015). doi:10.1093/bioinformatics/btv145 Medline

48. M. I. Love, W. Huber, S. Anders, Moderated estimation of fold change and dispersion for RNA-seq data with DESeq2. *Genome Biol.* **15**, 550 (2014). doi:10.1186/s13059-014-0550-8 Medline

49. E. Lund, A. R. Oldenburg, P. Collas, Enriched domain detector: A program for detection of wide genomic enrichment domains robust against local variations. *Nucleic Acids Res.* **42**, e92 (2014). doi:10.1093/nar/gku324 Medline

50. A. F. A. Smit, R. Hubley, P. Green, RepeatMasker Open 4.0, 2013–2015. www.repeatmasker.org.

51. F. Ramírez, F. Dündar, S. Diehl, B. A. Grüning, T. Manke, deepTools: A flexible platform for exploring deep-sequencing data. *Nucleic Acids Res.* **42**, W187–W191 (2014). doi:10.1093/nar/gku365 Medline

52. A. R. Quinlan, I. M. Hall, BEDTools: A flexible suite of utilities for comparing genomic features. *Bioinformatics* **26**, 841–842 (2010). doi:10.1093/bioinformatics/btq033 Medline

53. L. Wang, S. Wang, W. Li, RSeQC: Quality control of RNA-seq experiments. *Bioinformatics* **28**, 2184–2185 (2012). doi:10.1093/bioinformatics/bts356 Medline

54. D. Kim, G. Pertea, C. Trapnell, H. Pimentel, R. Kelley, S. L. Salzberg, TopHat2: Accurate alignment of transcriptomes in the presence of insertions, deletions and gene fusions. *Genome Biol.* **14**, R36 (2013). doi:10.1186/gb-2013-14-4-r36 Medline

55. Y. Liao, G. K. Smyth, W. Shi, featureCounts: An efficient general purpose program for assigning sequence reads to genomic features. *Bioinformatics* **30**, 923–930 (2014). doi:10.1093/bioinformatics/btt656 Medline

56. B. R. Graveley, A. N. Brooks, J. W. Carlson, M. O. Duff, J. M. Landolin, L. Yang, C. G. Artieri, M. J. van Baren, N. Boley, B. W. Booth, J. B. Brown, L. Cherbas, C. A. Davis, A. Dobin, R. Li, W. Lin, J. H. Malone, N. R. Mattiuzzo, D. Miller, D. Sturgill, B. B. Tuch, C. Zaleski, D. Zhang, M. Blanchette, S. Dudoit, B. Eads, R. E. Green, A. Hammonds, L. Jiang, P. Kapranov, L. Langton, N. Perrimon, J. E. Sandler, K. H. Wan, A. Willingham, Y. Zhang, Y. Zou, J. Andrews, P. J. Bickel, S. E. Brenner, M. R. Brent, P. Cherbas, T. R. Gingeras, R. A. Hoskins, T. C. Kaufman, B. Oliver, S. E. Celniker, The

developmental transcriptome of *Drosophila melanogaster*. *Nature* **471**, 473–479 (2011). doi:10.1038/nature09715 Medline

57. F. Ramirez, V. Bhardwaj, J. Villaveces, L. Arrigoni, B. A. Gruening, K. C. Lam, B. Habermann, A. Akhtar, T. Manke, High-resolution TADs reveal DNA sequences underlying genome organization in flies. bioRxiv 115063 (2017). doi:10.1101/115063

58. B. Schuettengruber, N. Oded Elkayam, T. Sexton, M. Entrevan, S. Stern, A. Thomas, E. Yaffe, H. Parrinello, A. Tanay, G. Cavalli, Cooperativity, specificity, and evolutionary stability of Polycomb targeting in *Drosophila*. *Cell Rep.* **9**, 219–233 (2014). doi:10.1016/j.celrep.2014.08.072 Medline

59. E. A. Carrington, R. S. Jones, The *Drosophila* Enhancer of zeste gene encodes a chromosomal protein: Examination of wild-type and mutant protein distribution. *Development* **122**, 4073–4083 (1996). Medline

60. B. Gaertner, J. Johnston, K. Chen, N. Wallaschek, A. Paulson, A. S. Garruss, K. Gaudenz, B. De Kumar, R. Krumlauf, J. Zeitlinger, Poised RNA polymerase II changes over developmental time and prepares genes for future expression. *Cell Rep.* **2**, 1670–1683 (2012). doi:10.1016/j.celrep.2012.11.024 Medline